Small Brains, Smart Machines: From Fly Vision to Robot Vision and Back Again

Nicolas Franceschini

Small Brains, Smart Machines: From Fly Vision to Robot Vision and Back Again

This paper reviews the design and construction of small insect-like robots that navigate and control their motion using biologically inspired visual strategies and circuits designed based on knowledge from computational neuroscience.

By Nicolas Franceschini

ABSTRACT | Neurobiological and neuroethological findings on insects can be used to design and construct small robots controlling their navigation on the basis of bio-inspired visual strategies and circuits. Animals' visual guidance is partly mediated by motion-sensitive neurons, which are responsible for gauging the *optic flow*. Although neurons of this kind were discovered in vertebrates' and invertebrates' visual systems more than 50 years ago, the principles and neural mechanisms involved have not yet been completely elucidated. Here, first, I propose to outline some of the findings we made during the last few decades by performing electrophysiological recordings on identified neurons in the housefly's eye while applying optical stimulation to identified photoreceptors. Whereas these findings shed light on the *inner processing structure* of an elementary motion detector (EMD), recent studies in which the latest genetic and neuroanatomical methods were applied to the fruitfly's visual system have identified some of the neurons in the visual chain which are possibly involved in the *neural circuitry* underlying a given EMD. Then, I will describe some of the proof-of-concept robots that we have developed on the basis of our biological findings. The 100-g robot OCTAVE, for example, is able to avoid the ground, react to wind, and land autonomously on a flat terrain without ever having to measure any state variables such as distances or speeds. The 100-g robots OSCAR 1 and OSCAR 2 inspired by the microscanner we discovered in the housefly's eye are able to stabilize their body using mainly visual means and track a moving edge with hyperacuity. These robots react to the optic flow, which is sensed by miniature optic flow sensors inspired by the housefly's EMDs. Constructing a ''biorobot'' gives us a unique opportunity of checking the soundness and robustness of a principle that is initially thought to be understood by bringing it face to face with the real physical world. Bio-inspired robotics not only help neurobiologists and neuroethologists to identify and investigate worthwhile problems in animals' sensory–motor systems, but they also provide engineers with ideas for developing novel devices and machines with promising future applications, in the field of smart autonomous vehicles and microvehicles, for example.

KEYWORDS | Angular velocity control; animal behavior; automatic control; bicycles; bio-inspiration; biological control systems; biological neural networks; biological system modeling; biorobotics; cybernetics; micro-air vehicles; micro-optics; motion detection; robotic visual systems; sensory–motor control systems; space vehicles; systems biology; unmanned aerial vehicles

NOMENCLATURE

OF	Optic flow.
EMD	Elementary motion detector.
HR scheme	Hassenstein–Reichardt scheme.
LPTCs	Lobula plate tangential cells.

I. FOREWORD

When studying electronics at the Polytechnic Institute in Grenoble, France, in 1964, I was extremely impressed when Prof. Jean Moussiegt showed me a paper published in the *Proceedings of the IRE*, in which the authors claimed that animals are equipped with visual neurons capable of detecting motion [1]. Might animal brains, or perhaps even

Manuscript received November 15, 2013; revised March 3, 2014; accepted March 17, 2014. Date of publication April 24, 2014; date of current version April 28, 2014. This work was supported by the Max-Planck Society (Germany); the Aix-Marseille Université, CNRS, ISM, UMR 7287 (France); the French National Research Agency (ANR); the French Government Defense Procurement Agency (DGA); and the European Union under Grants Codest, Esprit,TMR, and IST-FET.
The author is with the Biorobotics Lab, Institute of Movement Science, Aix-Marseille University and UMR CNRS 7287, Marseille 13288, Cedex 9, France (e-mail: nicolas.franceschini@univ-amu.fr).

my own brain, contain circuits just like those we were learning about in the field of electronics? This shock of discovery actually prompted me to switch from electronics and control theory to neuroscience and behavioral science. I had no idea at that time that intensive efforts would still be continuing 50 years later on elucidating the detailed principles underlying the neural processes involved in humans' and animals' motion perception and visuo–motor control [2]–[6]. Shortly afterwards, I read that a model accounting for motion detection based on an autocorrelation principle had been developed in Germany [7]. Armed with my recent B.E. report on "analog multipliers," I knocked at Werner Reichardt's door, in what was soon to become the Max-Planck Institute for Biological Cybernetics. During my 13-year stay in Tübingen, Germany, I had the great privilege of benefiting from the immense devotion, knowledge, and iconoclastic thinking of my three mentors, Karl Götz, Kuno Kirschfeld, and Dezsö Varju. Prof. Varju passed away recently and it is an honor for me to dedicate this paper to his memory.

II. INTRODUCTION

When pondering what it means to "understand" a complex information processing system such as a brain, Marr and Poggio [8] defined four levels of description: 1) the computational level of description; 2) the algorithmic or functional level; 3) the mechanisms; and 4) the hardware. The first three levels can be used to describe a system in abstract terms, regardless of the machinery, whereas the fourth level is about the biological components and networks, which range from nanometer-sized synaptic junctions between neurons to long connections between brain regions [6], [9]. The use of these complementary levels of analysis and understanding in various combinations has been illustrated remarkably in the field of neuroscience in general and in the analysis of visual motion in particular. An excellent example is provided by the elementary motion detector (EMD) present in insects' compound eye, a subject on which a plethora of studies have focused since the pioneering behavioral work by Hassenstein and Reichardt, who presented the influential "correlation model" of motion detection [7], [10]–[14].

Motion detection is as relevant to insects' visual guidance as it is to human visuo–motor control [2], [3], [15], [16]. We have long known that insects navigate by processing the optic flow (OF), which describes the speed of images streaming across their retina as the consequence of their own movements [17], [18]. The OF is a vector field where each vector describes the local angular speed ω of each contrasting feature present in the field of view (FOV). Recent studies have shown that honeybees' speed depends on dorsal as well as lateral, ventral, and frontal OFs [19], which help them delve under foliage and flowers in search of nectar. Flies rely on OF cues as well to venture into highly unpredictable environments, often attaining a level of agility [20]–[22] that greatly outpasses that of both vertebrate animals and present-day aerial robots. Flies are capable of autonomous takeoff, dynamic stabilization, hovering, ground avoidance, collision avoidance with stationary and nonstationary obstacles, tracking mates and intruders, intercepting preys, docking, landing, decking on nonstationary substrates, and more. Flies are certainly rather objectionable in many ways, but these humble creatures show that it is definitely possible to achieve 3-D navigation at up to 1000 body lengths per second using quite modest processing resources. This behavioral feat, which is achieved without any tethers to supercomputers and external power supplies, tickles roboticists' imaginations. Some research groups have started constructing seeing micro-air vehicles (MAVs) (e.g., [23]–[27]). Others have started producing tiny flapping-wing MAVs (e.g., [28]–[34]). The latter are remotely controlled, however, and lack the impressive sensory–motor control and autonomous power resources of which insects can boast.

In this review, I will first describe various attempts to analyze the fly visual system and its motion-sensitive neurons. The fly is one of the best animal models currently available for studies on motion perception. I will then describe the neuromorphic EMDs that we built, and various robots equipped with these EMDs. The aim of the former studies was to dig up a basic information processing scheme. The aim of the latter studies was to build proof-of-concept robots that would emulate some of the visuo–motor control tricks used by insects to negotiate complex environments, while at the same time possibly giving some feedback about the real biological situation [35]. This approach, which consists in performing not only computer simulations but also real physical hardware simulations (e.g., [36]–[60]; see also the reviews in [61]–[86]) is sometimes called "synthetic modeling" [87]. When it is attempted to stick to the analog mode of processing dear to animals' nervous systems using either very large scale integration (VLSI) or classical analog circuits (e.g., [87]–[90]), the approach is known as "neuromorphic engineering" [88], [91], [92]. This approach, which we started to use in 1985, relates to the now fast expanding fields of bionics and biomimetics [74], [85], [86], one of the main thrusts of which is to build autonomous mobile vehicles inspired by animals' sensory and motor systems.

I will also describe fruitful returns to biology resulting from the use of the synthetic modeling approach and conclude by discussing how insect-inspired principles of visual guidance might be usefully applied to the MAVs and micro-space vehicles (MSVs) of the future, which, like insects, will not be allowed to carry any of the cumbersome, heavy, energy-consuming avionic sensors usually installed on conventional aircraft.

III. THE FLY'S OPTOMOTOR RESPONSE

Flies, like other insects, show an interesting, well-documented visuo–motor reaction known as the optomotor

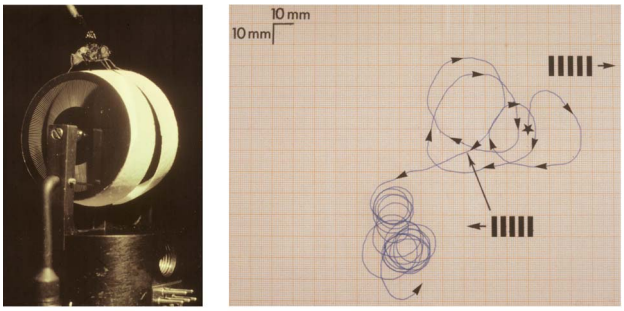

Fig. 1. *(a) The Mark I Fly Bicycle (1973) constructed for analyzing insect's optomotor responses quantitatively. The housefly Musca domestica was tethered to a solder wire with a drop of bee wax and placed gently on its bicycle by means of a micromanipulator until the right legs were driving the right tread wheel and the left legs were driving the left tread wheel. The ensuing rotation of each 80-mg Styrofoam wheel, the pointed axle of which was mounted between V-shaped sapphire bearings, was monitored at high resolution via a light barrier composed of 200 thin (100-μm width) spokes crossing the microbeam originating from an optical fiber (80-μm diameter). (b) "Virtual trajectory" of the housefly on its bicycle, as recorded on the original piece of parchment, when the two eyes were presented frontally with a grating moved horizontally on an oscilloscope screen. The animal reacted by adopting a tightly curved trajectory, the direction of which immediately changed when the pattern was moved in the opposite direction (thin arrow). This 20-s trajectory was computed online from the pulse trains delivered by the two tread wheels, each of which generated about 200 impulses/s ("spikes") when the fly was walking straight ahead at a speed of 10 cm/s.*

response. This is a turning response evoked by the perceived motion of the visual environment. This response based on these insects' great sensitivity to directional motion [93]–[96] is thought to stabilize their orientation with respect to the environment. A number of precision devices have been constructed to assess the optomotor response of a walking insect under "open-loop" conditions, i.e., by abolishing the visual feedback loop between the animal and its environment. Some classical examples of these devices are Hassenstein's "Spangenglobus" ("Y-maze globe") [97]) and Buchner's miniature air-supported ball [95], both of which were used in pioneering studies on insects' optomotor systems and continued to be used for several decades (e.g., [98] and [99]). Fig. 1(a) shows yet another "virtual reality machine," the fly bicycle, which I built in 1973. While clamped in space, a head-fixed insect can be presented with specific optical stimuli that will not be perturbed by the animal's body or head movements. The virtual trajectory produced by a tethered housefly in response to a drifting grating presented in its frontal FOV is shown, for example, in Fig. 1(b). A simple method of assessing the insect's turning tendency consisted in integrating the "spikes" generated by each bicycle wheel.

Flies' optomotor response is one of the rare kinds of animal visuo–motor behavior that have ever been pinned down to individual, identified neurons. Many lines of evidence (e.g., [100]–[103]) have shown that flies' optomotor response is mediated by a remarkable set of uniquely identifiable, directionally selective motion-sensitive neurons [Fig. 5(b)], the activity of which has been well documented and even started to be recorded during the performance of optomotor walking or flying tasks by a tethered fly [99], [104].

IV. THE FLY'S COMPOUND EYE

The fly's compound eye is a real treasury of integrated optronics, neuronics, and nanomechatronics, as we will see in this section and in Section V. The eye of the *Drosophila* fruitfly [Fig. 15(d)] has for long served as a model system for understanding many aspects of cell differentiation (see, e.g., [105]). Today, the use of genetic blocking methods on known cell types is beginning to revolutionize our detailed understanding of motion detection processes down to the single-cell level [106]–[108], as described in Section V-D. In the housefly—the model system I will focus on here—each compound eye consists of a curved array of about 3000 adjacent ommatidia, separated by an angle $\Delta\varphi$ of about 2°. The facet lenslet of each ommatidium focuses light onto a small set of photoreceptor neurons which act like quantum transducers. The phototransduction process [109] makes a cell depolarize when it is exposed to light [Fig. 2(c), top traces]; its total dynamic range is no greater than 70 mV. Each cell has its own visual axis [Fig. 2(b)] and directivity [Fig. 3(a)]. Step-by-step processing of the photoreceptor signals occurs in four successive ganglia ("neuropils") forming the lamina, medulla, and lobula complex [see Fig. 5(a)] [110], [111]. Each ganglion consists of a periodic array of repeat units (called cartridges in the lamina, and columns further down). A single medulla column may harbor approximately 40 columnar neurons [110]–[112]. There exists a one-to-one correspondence between the array of ommatidia, the array of lamina cartridges, and the array of medulla columns, and each of these arrays of repeating neural modules projects to the next one in a highly ordered ("retinotopic") fashion [110].

Each eye samples the world with an omnidirectional array of visual sampling units forming a remarkably hexagonal lattice, whose precise orientation can be mapped in the far field by pointing a telescope at the compound eye [125]. A striking division of labor occurs at this peripheral level, as each of these visual sampling units contains two sets of coaxial photoreceptors subserving different patterns of behavior [96], [126], [127].

- The two "inner" photoreceptor cells R7 and R8 are arranged in tandem [Fig. 2(b), bottom right] and, therefore, have a common visual field [Fig. 3(a)]. They show various spectral sensitivities scattered across the retinal mosaic, as attested by the various R7 autofluorescence colors [Fig. 2(a)] [114], [116].

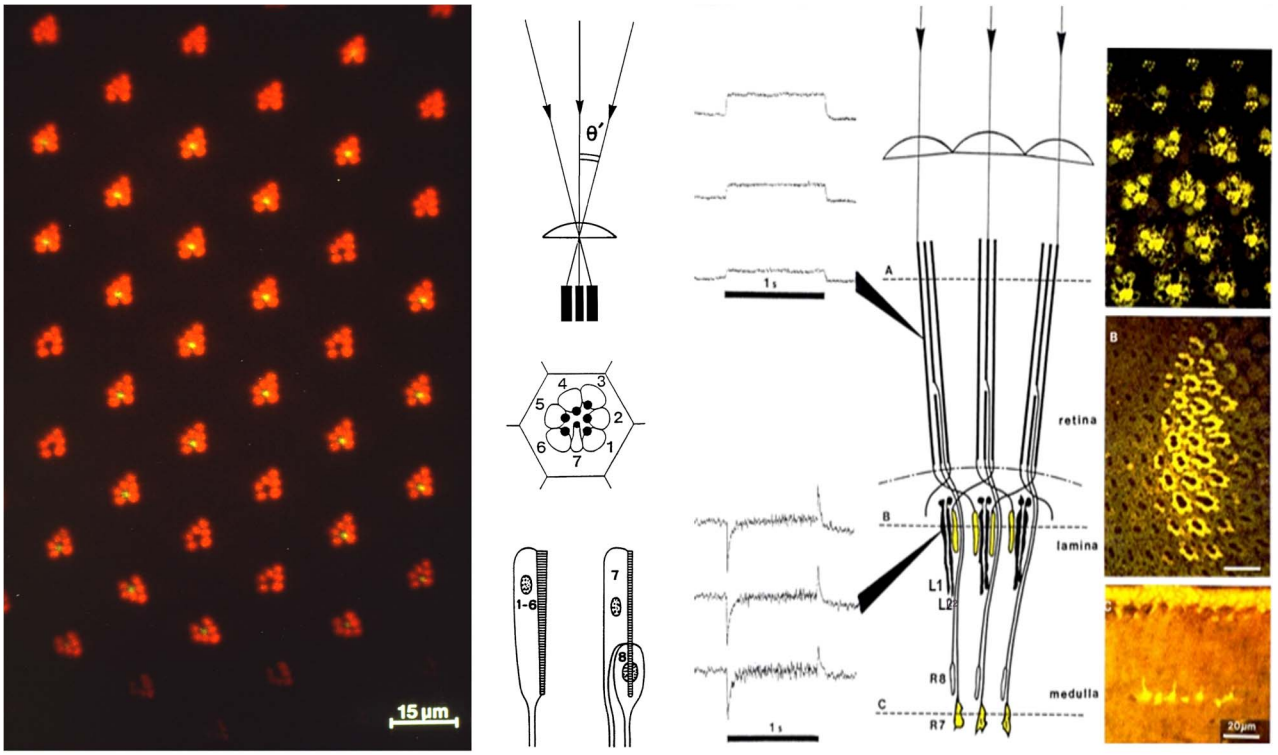

Fig. 2. *Housefly photoreceptors and second-order neurons: functional structure and electrical responses. (a) Frontal–dorsal part of the right retina of a male housefly observed in vivo under epi-fluorescence microscopy (blue excitation) using corneal neutralization with water immersion [113] and an aperture filtering technique. The various autofluorescence colors of the "inner" cells (R7) reflect their various spectral sensitivities [114]–[116] and contrast with the homogeneous red emission of the "outer" cells (R1–R6); some red-fluorescing R7s are also seen here in the top part: they belong to the love spot of the male eye (see Section IV). (b) Visual axes, cross section of an ommatidium, numbering, and structure of the photoreceptors in a longitudinal section. (c) and (d) Each of the eight receptor cells responds to a 1-s pulse of light with a depolarization that increases logarithmically with the intensity (responses shown here at one-decade intensity intervals) [118]. By contrast, the two large monopolar cells L1 and L2 respond to their six photoreceptor inputs with a transient negative signal at light ON and a transient positive signal at light OFF [119]–[121]. (e) Semi-thin sections through the retina, lamina, and medulla showing the stained axonal projections from various photoreceptor types R1–R6 and R7. The terminals of all the R1–R6 photoreceptors that received light from the epi-fluorescence microscope's objective show up in yellow in the lamina (e_b) due to their photopermeabilization to the (extracellularly applied) dye Lucifer yellow [122], [123]. In the core of each lamina cartridge, the monopolar cells L1 and L2 stand out distinctly in black, surrounded by six yellow R1–R6 terminals (stemming from six neighboring ommatidia). (e_c) yellow stained R7's terminals in the medulla. (Data in (a) and (b) were originally published in [124]; recordings in (c) were made by M. Wilcox; data in (d) to (e) were originally published in [123].)*

R7 and R8 participate in color vision, with no less than four different spectral sensitivities [115], [105], [118], [128]. They project directly to the second optic ganglion, namely, the medulla [see, e. g., the yellow-stained axonal terminals of R7 cells in Fig. 2(e_c)], where the color pathway is split into various columns receiving inputs from either "pale" or "yellow" R7 and R8 cells [129].

- The "outer" six photoreceptors (R1–R6) participate in motion detection, in particular, and are responsible for the optomotor response [14], [95], [98], [126], [127]. Consistent with this function, where contrast sensitivity is at a premium, R1–R6 photoreceptors constitute a high sensitivity ("scotopic") system [132] due to their wider FOV (Fig. 3(a) and [117]), their broadband, UV-enhanced spectral sensitivity [133], and their exquisite neural projections onto the underlying optic ganglion (the lamina), on which the "neural superposition principle" is based. This wiring pattern is such that six R1–R6 receptors looking in the same direction in space [two of them are depicted in Fig. 2(d_a) with their parallel visual axes] but belonging to neighboring ommatidia, send their axons to the same cartridge in the lamina [134]–[136], where they convey their graded signal to a few second-order neurons, in particular, the pair of large monopolar cells L1 and L2 [the black profiles visible in Figs. 2(d), 2(e_b), and 3(e)]. Neural addition of these six independent

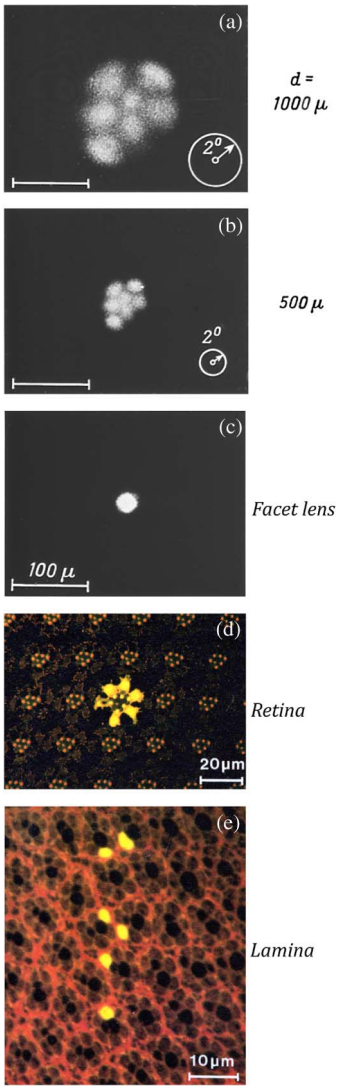

Fig. 3. *Optoneural projection of the FOV of a single ommatidium onto the array of cartridges in the housefly lamina. (a) and (b) Microphotographs of the receptive field of each photoreceptor cell of an ommatidium, obtained by transilluminating the whole head ("antidromic illumination") while covering a single facet (c) with a circular metallic microdiaphragm [132]. The picture in (a) is a magnified and inverted real image of the seven photoreceptor front ends [Fig. 2(a)]. Each photoreceptor has a bell-shaped FOV [as schematized in Fig. 9(a)], which determines its contrast transfer properties [94]. The FOV of the inner cell R7 [prolonged by R8; see Fig. 2(b), bottom part] is about half that of the outer R1–R6 photoreceptors. (d) and (e) Neural projection of photoreceptors R1–R6 of an ommatidium, obtained by illuminating a single facet [as in Fig. 6(a), inset] through an epi-fluorescence microscope and photopermeabilizing the photoreceptors to the dye Lucifer yellow [122]. Each stained axon projects to its corresponding lamina cartridge, as predicted by the principle of neural superposition [cf. Fig. 2(d)]. In (e), the two monopolar cells L1 and L2 show up in the form of black profiles in the core of each cartridge [as in Fig. 2(e_b)]. The image inversion produced by the facet lens is "compensated for" by the tortuous photoreceptor axonal wiring (vividly described by [134] and accurately drawn in [135]) so that the pattern formed by the six yellow axons in the lamina (e) is congruent to the pattern formed by the six FOVs (a). (Data in (a)–(c) are from [132]; data in (d) and (e) are from [122].)*

signals (corresponding to the same point in space) results in a signal-to-noise ratio enhancement by a factor of $\sqrt{6}$ [137], [138], and hence in an improved sensitivity, without any loss of acuity [132], [136]. L1 and L2 both respond to a light step with a similar transient signal, which looks like a sign-inverted high-pass-filtered version of their photoreceptor inputs [see Fig. 2(c), bottom traces] [119], [139]. This early temporal filtering process is highly suitable for extracting information about the contrast (Rev. [120]).

A surprising version of this wiring scheme occurs in the dorsal acute part (the "fovea") of the male housefly's eye, where a "love spot" [116], [140] drives male-specific neurons [141] presumably involved in female chasing activities [142] (see also [143]). This love spot is distinguished by special R7 photoreceptors [the red fluorescing R7s visible in the upper part of Fig. 2(a)]. These R7s have the same spectral sensitivity as their six neighbors and also contribute to the process of "neural superposition" [116], thus enhancing the signal-to-noise ratio even more (by a factor of $\sqrt{7}$ instead of $\sqrt{6}$) in this male-specific neural pathway dedicated to a really great cause [111], [128].

One aspect of the neural superposition principle is that each photoreceptor R1–R6 of an ommatidium sends its axon to a different cartridge in the lamina [135]. Fig. 3 presents a direct opto-neural projection onto the lamina of the visual field of the R1–R6 photoreceptors from a single ommatidium. Each of the seven visual fields (photographed at two different distances) has a bell-shaped cross section with a half-width—termed "acceptance angle"—of the order of 2° [117]. Each visual field expresses the directivity of the cell and can be said to constitute the far-field radiation pattern of a receiving microantenna, with a gain of approximately 37 dB in the case of the outer R1–R6 cells [125]. This highly accurate retina–lamina projection pattern allowed us to stimulate two neighboring cartridges, in order to analyze the inner processing structure of an isolated EMD (Sections V-B and C).

A fast intracellular pigment migration mechanism prevents all the photoreceptor cells from being overstimulated [145]–[147]. This is a nanomechanism where strongly absorbing granules (with a diameter of ≈100 nm) move up intracellularly toward the rhabdomere (the rod-like light sensing organelle of the photoreceptor cell), which acts as a dielectric waveguide [113]. By interacting with the evanescent wave [145], the granules reduce the effective light flux destined for the cell by as much as 100-fold [121], [146], [148]. This mechanism is an "intracellular pupil" acting independently within each photoreceptor cell in a matter of seconds [146], [147]. The underlying processing scheme was found to be a multiplicative feedback ("automatic gain control") system [149]. Light absorption by the visual pigment results in an increase in the intracellular calcium concentration [150],

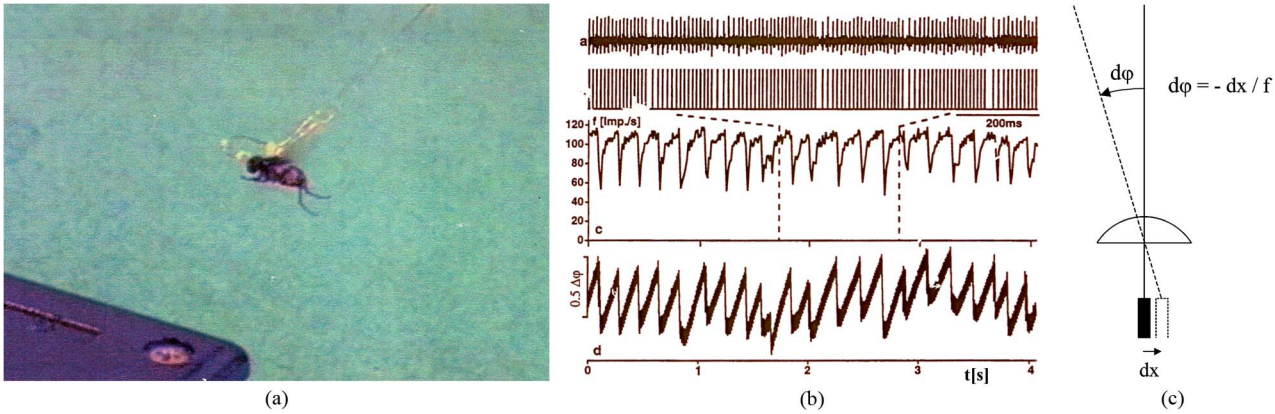

Fig. 4. *(a) Flying housefly on the leash. The insect was flying freely at the tip of a double enameled copper wire (20-μm diameter, 0.4-m length) serving as a differential electrode (picture taken from a video film). (b_a) In-flight recording of the spikes generated by the MOT eye muscle. (b_b) Unit pulses triggered by the individual spikes showing the periodic dropouts. (b_c) Instantaneous spike frequency plot showing that about five times per second, the high frequency (approximately 110 Hz) of the MOT spontaneously dropped by about half. (b_d) and (c) The periodic dip in the firing rate caused periodic displacements dx of the photoreceptors in the focal plane of each facet lenslet, resulting in periodic angular displacements dφ of the visual axes. (The data in (b) are from [155].)*

which in turn activates a "nanomotor" based on the motor protein Myosin-V [151], which gradually closes the "pupil" at luminances above 3 cd/m^2 [147]. The pupil mechanism was shown to prevent saturation and extend the range of light intensities over which the receptors operate with a near-maximal signal-to-noise ratio [121].

One particularly intriguing finding made here was that the visual axes of the ommatidia are not stationary. We have observed that the coordinated action of two eye muscles, the *Musculus orbito-tentorialis* (MOT) [152], [153] and the *Musculus orbito-scapalis* (MOS) [154], shifts the photoreceptor mosaic located below the facet mosaic, thus concomitantly shifting the photoreceptors' line of sight [Fig. 4(c)] [154]. Most surprisingly, the retina is thereby made to perform repetitive microscanning movements with a frequency of 5–7 Hz when the animal is flying, as shown by the recordings made from the MOT in a quasi free-flight situation [Fig. 4(a) and (b)] [155]. A retinal microscanner of this kind was incorporated into the eye of several miniature robots constructed at our laboratory (Sections IX and X), which revealed major benefits of a retinal microscanner and served at the same time to test functional hypotheses about flies' eye muscles (see the end of Section IX).

V. THE FLY'S EMDs

A. The Systems Approach and the Cellular Approach

In the 1950s, a phenomenological model for motion perception was developed by Hassenstein and Reichardt (HR) to account for the optomotor responses of the Chlorophanus beetle [10], [12]. In the HR model for an EMD, the signals from two adjacent ommatidia were multiplied after one of them had been delayed. The result of the multiplication itself was low-pass filtered. Since multiplying a signal by its delayed version followed by low-pass filtering is called correlation, the HR model is often called the HR correlation detector [12]–[14], [157]. To be complete, the HR model assumed the existence of two mirror-symmetric EMD subunits of this kind, the outputs of which were subtracted from each other, thereby increasing the direction selectivity.

In the 1980s, we used a micro-optical stimulation technique specially designed for investigating the inner processing structure of a single EMD. This unusual method of stimulation has never been used again on any animal for 25 years, but the main results obtained in this way [158] have stood the test of time and now benefit from a revived interest [106]–[108]. The model we arrived at still fits with the HR model but unveiled essential details about the inner processing structure. Sections V-B and C therefore summarize the work we performed with single-cell recording and single photoreceptor stimulations. Section V-D deals with some very recent studies involving the use of innovative techniques, which not only corroborate our own results but also relate the findings we obtained at systems level to the cellular data available.

The results we obtained under single-cell stimulation conditions greatly influenced our subsequent research, as they suggested a means of building neuromorphic EMDs (Section VI), which were soon to be mounted onboard various proof-of-concept robots capable of performing various tasks on the basis of insect-inspired OF cues (Sections VII–X).

During the last few decades, it has been clearly established that the lobula plate of the fly's compound eye [Fig. 5(a)] is a visual motion processing center devoted to both head and body stabilization and visual guidance. All

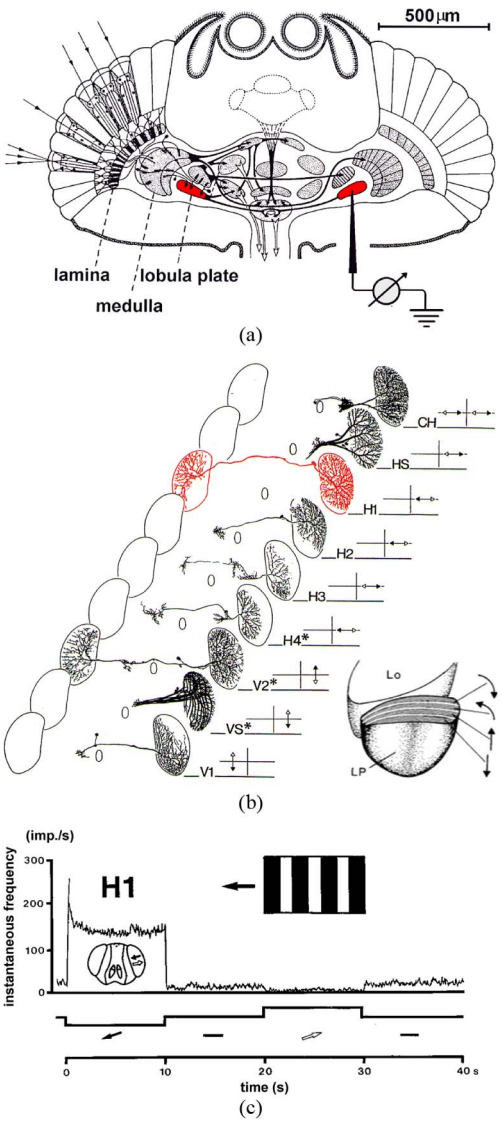

Fig. 5. *(a) Schematic horizontal section through the head of a fly, showing the visual centers located beneath the facet array. By introducing a microelectrode into the lobula plate, it is possible to record the electrical activity of any one of the 50 identifiable motion-sensitive neurons present in this ganglion. (b) An "exploded view" of 23 of the wide-field LPTCs of the right eye along the median axis of the head. Each of these neurons is not only motion sensitive but also directionally selective (its preferred direction is symbolized by the black arrow in one of the visual hemifields). A symmetric set of neurons is found on the other side of the head. Inset: horizontal cut through the right lobula and lobula plate. In each eye, the lobula plate accommodates the LPTCs in four distinct layers, each of which is specialized in one of the four cardinal directions of motion: front-to-back, back-to-front, upwards, and downwards—an organization reminiscent of the vertebrate retina [182]. (c) Response of the H1 neuron [red in (b)] to the motion of a grating (contrast $m = 0.85$) moving horizontally forward (in the "preferred direction") and backward (in the "null direction") in the FOV of the left eye. The plot shows the spike frequency profile (post-stimulus time histogram, $n = 32$). (Data in (a) are adapted from [183], data in (b) are adapted from [164], inset is reproduced with permission from [181], and data in (c) are from [131].)*

the neurons lurking in this ganglion [110], [159] respond to directional motion [160]–[162] and serve as OF sensors [161], [164]–[166]. Twenty three of these (approximately 50) lobula plate tangential cells (LPTCs) present on each side of the blowfly's head are shown in Fig. 5(b) published in the Hausen's pioneering studies [161], [164]–[166]. Since all these neurons are uniquely identifiable, a given experiment can be repeated on the same neuron in different animals. These neurons are all wide-field collator neurons giving off many dendrites that receive outputs from hundreds of EMDs, all awaiting the occurrence of local motion within an extensive FOV [163]. The neuronal activity of these LPTCs, like that of any other sensory neuron, is affected by noise sources within and outside the nervous system, which can compromise their reliability. A recent study has attempted to study motion perception from the perspective of ideal observer theory. The authors were able to assess the effect of noise at major stages of the fly's visual motion pathway, and dealt both with external signal variability and internal variability up to the motor response [168].

The H1 neuron [red in Fig. 5(b)]—the neuron I will focus on here—is most sensitive to horizontal, back-to-front motion on the ipsilateral eye and codes pattern velocity in terms of its spike rate [161], [169], [170]. Fig. 5(c) shows the response of H1 to the horizontal motion of a square-wave grating [131]. During the first 10 s, the neuron was strongly excited by back-to-front motion (i.e., motion in the "preferred" direction). From 20 to 30 s, it was strongly inhibited by front-to-back motion (i.e., motion in the "antipreferred," or "null" direction). The quasi-disappearance of spikes which occurs in response to front-to-back motion corresponds to the actual situation experienced by a fly during straightforward flight [171]. Although most of the other LPTCs drive descending neurons controling leg, wing, and head movements [172]–[175], the H1 neuron transmits its signal to the contralateral lobula plate, where the spikes can be reliably recorded with a microelectrode, while preserving the optics of the eye on the stimulated side [Fig. 5(a) and (b)].

Presenting an eye with a drifting sine, random or square-wave grating [Fig. 5(c)] is a classical method of analyzing animal and human motion detection. Another method consists in stimulating the retina with moving spots or bars (e.g., [176]) or contrasting edges (e.g., [177]). Alternatively, one can present the eye with two neighboring steady spots or slits sequentially (e.g., [177]) in order to elicit the kind of "apparent motion" that Exner experienced early in 1875 [178]. All these methods of stimulation have been successfully used to characterize the performances of arrays of motion detectors (their spatial extent, speed selectivity, temporal frequency dependence, contrast sensitivity, response dynamics, motion adaptation, etc.) in both vertebrates and invertebrates. All these methods suffer, however, from stimulating a large (usually

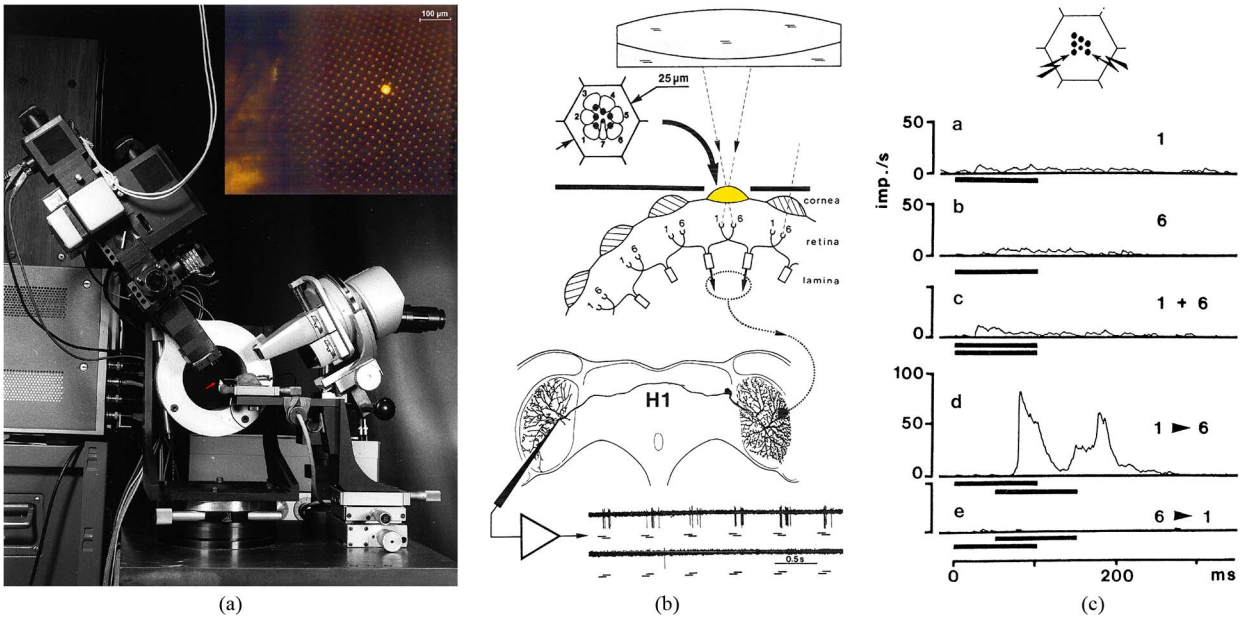

Fig. 6. *(a) Triple-beam, rotating incident-light "microscope–telescope," with which two identified photoreceptors (R1 and R6) in the ommatidium of interest (inset) can be stimulated sequentially with 1-μm light spots so as to simulate a horizontal motion ("apparent motion"). The tethered housefly can be seen at the tip of the red arrow. Inset: the facet selected (diameter $\cong$ 25 μm) received light along the visual axes of R1 and R6 [see (b) and Fig. 3(a)]. (b) Principle of the experiment and spike responses of the H1 neuron to repeated sequences of light flashes or steps. Successively illuminating the two neighboring photoreceptors R1 and R6 amounted to stimulating two neighboring cartridges in the lamina [see Fig. 3(e) and 7(a) and (b)]. These in turn drive an EMD (dotted ellipse) conveying its outputs (dotted line) retinotopically to the dendritic arbor of H1. Bottom part: a conspicuous double burst of spikes was elicited by illuminating R1 and R6 with a light sequence simulating motion in the preferred direction (R1 then R6, top trace), and a quasi absence of spikes was observed with the opposite sequence (R6 then R1, bottom trace) (flash duration 100 ms, interstimulus interval 50 ms). (c) H1 firing rate (averaged over 100 stimulus presentations) evoked in response to single-cell or two-cell stimulation with the same sequence as in (b) [131]. Again, a clear-cut response was evoked only with the sequence simulating motion in the preferred direction (R1 then R6). (Data in (a) are adapted from [158], data in (b) are adapted from [124], and data in (c) are adapted from [131].)*

undefined) number of (usually unidentified) photoreceptors which, in turn, drive tens or thousands of EMDs, not to mention the many additional visual interneurons which may interact with the EMDs (see, e.g., [179]). In view of the daunting complexity of the underlying neural hardware and its untold number of connections [110] (appaling updates were given in [130] and [179]), we searched for a method of stimulation that could be used to isolate an EMD and reveal its inner processing structure in a more direct way.

B. Teasing Out the Inner Processing Structure of an EMD

By adapting the micro-optical techniques we previously developed [125], we were able to record from the H1 neuron while stimulating two identified photoreceptors (R1 and R6) in a single ommatidium [see Fig. 2(a) and (b)] [131]. Exposing R1 and R6 to a sequence of illumination would activate two nearest neighboring cartridges in the lamina [see Fig. 3(d) and (e)], between which motion detection was expected to take place. My hope that the response signature of an EMD would then stand out from the H1 response was supported by the results obtained in a former study, in which a clear-cut optomotor response was triggered in the housefly using a (slightly different) method of single-cell stimulation [98]. With two identified input receptor neurons and one identified output neuron, the problem in hand amounted to a classical system identification problem.

The incident light stimulation instrument which I constructed for this purpose is a hybrid between a microscope and a telescope [Fig. 6(a)], where the main objective lens is quite simply the facet lens itself (diameter $\cong$ 25 μm, focal length $\cong$ 50 μm) [Fig. 6(a), inset] [158]. This instrument serves: 1) to select a given facet lens by projecting the real image of an optical mask onto it [Fig. 6(b), top]; 2) to select two out of the seven photoreceptors visible *in vivo* in the back focal plane of the facet lenslet; and 3) to stimulate these micrometer-sized photoreceptors (R1 and R6) successively with 1-μm light spots. This procedure, which simulates a micromotion occurring within the narrow FOV of the ommatidium selected [see Fig. 3(a)], amounts to exciting two neighboring cartridges [see Fig. 3(e)]. It turned out that H1

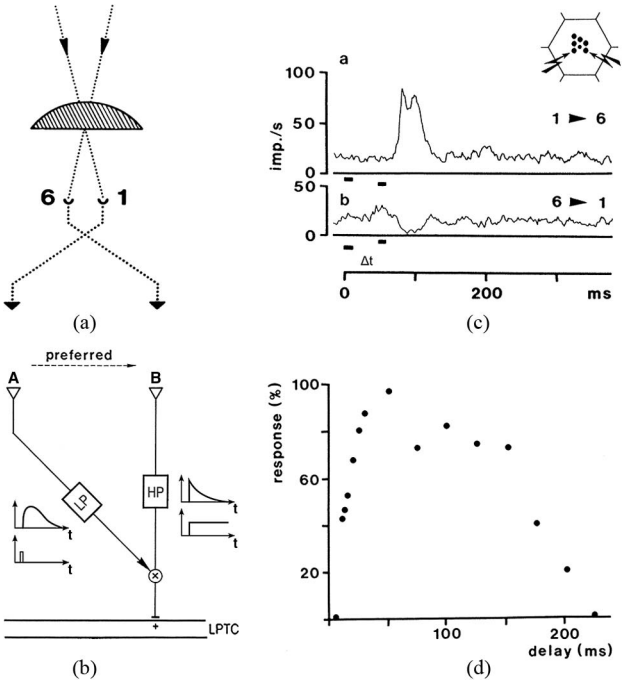

Fig. 7. *(a) Optical method used to drive the two input cartridges A and B of an EMD via single photoreceptor illumination [cf., Fig. 6(b) and 3(e)]. (b) Block diagram of the elaborate HR half-detector (sensing motion in the preferred direction) resulting from our microstimulation experiments. (b) Sequential illumination of the photoreceptors R1→ R6 drives the two cartridges A → B, producing "apparent motion" in the preferred direction, which conveys an excitatory signal (+) to the LPTC. The box in the left arm describes a second-order low-pass (LP) filter, the impulse response of which was measured in (d). The box in the right arm describes a first-order high-pass (HP) filter, the step response of which was measured in Fig. 8(a). (c) Response of H1 (spike instantaneous frequency) to a pair of brief (10-ms) flashes presented sequentially to the photoreceptors R1 and R6 (diameter ≅ 1 μm) of an ommatidium (inset) (spot diameter ≅ 1 μm, interstimulus interval Δt = 50 ms, repetition time = 500 ms, average n = 100). Note that the sequence simulating motion in the antipreferred direction (R6 → R1) inhibits H1: this suggests the existence of a coextensive, mirror-symmetric EMD half-detector driven by the same two cartridges B and A and sensing motion in the opposite direction. (d) Impulse response of the low-pass filter of the lateral facilitating arm in (b), elicited by presenting R1 and R6 with sequences of brief (10-ms) flashes with various interstimulus intervals (data are means of H1 recordings on nine houseflies). (Adapted from [158].)*

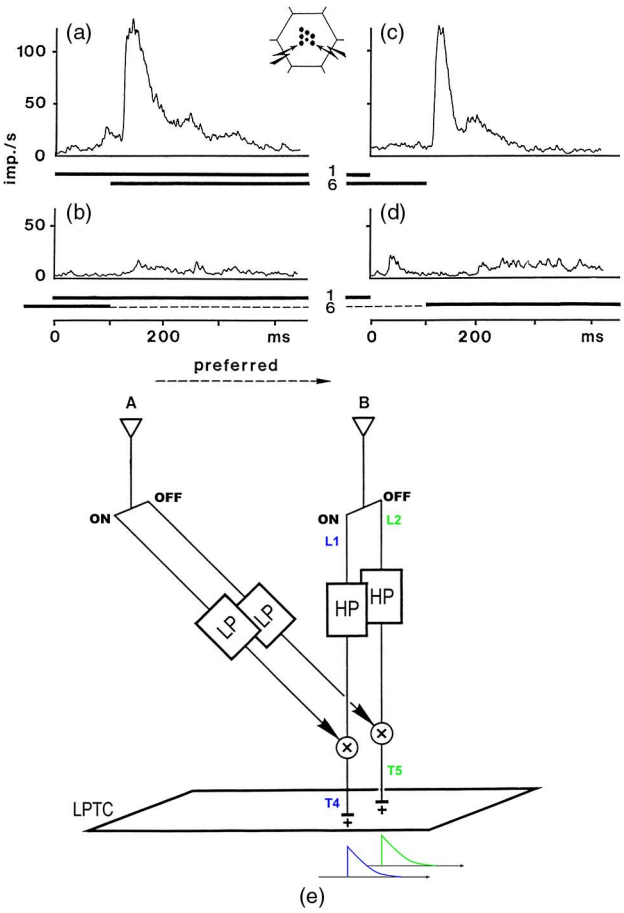

Fig. 8. *(a)–(d): H1 responses to mixed sequences of long-lasting light and dark pulses (spot diameter ≅ 1 μm) received by two single photoreceptors R1 and R6. Among the eight step sequences that can be produced by manipulating the sign and the delay of the changes of brightness delivered to R1 and R6, only the two sequences shown in (a) and (c) triggered a clear-cut response in H1 [158]. The latter sequences roughly simulate the motion of the leading edge (a) and trailing edge (c) of a bright object in the preferred direction [each response is the average response recorded in 100 sequence presentations; time between two sequences: 2000 ms; stimulation of R6 in (b) and R1 in (d) started at t = −1000 ms]. (e) (Black scheme): The responses shown in (a)–(d) suggest that the EMD half-detector responsible for the preferred direction is split into two subunits operating in parallel: an ON-EMD and an OFF-EMD which sense the motion of light edges and dark edges separately, and convey excitatory signals to H1 [158]. The twin EMD subunits represented here are those responding to the preferred direction only: both convey an excitatory signal to H1. The two exponentially decaying signals shown below symbolize the step responses of the ON- and OFF-EMD subunits, as observed in (a) and (c). (Colored letters): Recent experiments [107], [199] involving the genetic silencing of lamina L1 and L2 neurons suggested that the front end of these twin ON- and OFF-pathways may be the large monopolar cells L1 and L2. Motion sensitivity is conveyed down to the LPTC via the bushy cells T4 and T5 (see Section V-D), which were recently found to be strongly directionally selective [108]. (Data in (a)–(e) are from [~~125~~, Figs. 15 and 16]; top color letters L1 and L2 are based on [107] and [199]; bottom color letters T4 and T5 are based on [108].)*

responds by producing a prominent spike discharge provided the time elapsing between the two stimuli corresponds to motion in the preferred direction, and hardly responds at all when the sequence corresponds to motion in the antipreferred direction [see the two recordings at the bottom of Fig. 6(b)] [131].

It is worth noting that applying microstimulation to only 2 out of the 48 000 photoreceptor cells ($3000 \times 8 \times 2$) of the housefly's compound eyes elicited a marked response [the firing rate reached about 100 Hz, as shown in Figs. 6(c_d), 7(c) and 8(a) and (c)] in the H1

neuron, although each of the two lamina cartridges activated was running on only one of six inputs [compare Fig. 3(e) to Fig. 2(e_b)]. In the first place, this is consistent with the finding that stimulating only one of the six photoreceptors' inputs to one cartridge suffices to activate the postsynaptic cells L1 and L2 [138]. Second, this shows that the summation process which occurs in H1 is very nonlinear, in line with the early findings made upon stimulating H1 with drifting gratings of various sizes [164], [165].

Based on many experiments of this kind, in which sequences of light pulses or steps were applied to the two receptors, we gained step-by-step access to the dynamic components of an EMD, downstream of the two lamina cartridges A and B [triangles in Fig. 7(b)]. The conclusions we drew from these experiments on the EMD half-detector responsible for the preferred direction are briefly described here [Fig. 7(b)].

1) Illuminating a single photoreceptor, R1 or R6, or both simultaneously, elicited hardly any response in the LPTC [Fig. 6($c_{a,b,c}$)]. We are dealing here with a true directionally selective motion-sensitive detector, which is immune to synchronous stimulations on its two inputs.
2) Upon presenting R1 and R6 with an "apparent motion" stimulus (a sequence of 100-ms flashes), the first stimulus did not elicit any response [see Fig. 6(c_d)] but no doubt had an internal effect: it facilitated the response to the second stimulus. This experiment for the first time established the sequence-discriminating ability of an isolated EMD driving an LPTC [131]. The scheme we arrived at is presented in Fig. 7(b). The left arm is the facilitating arm. The right arm is the facilitated arm driving the LPTC with a positive (excitatory) signal.
3) The impulse response of the filter present in the facilitating arm (driven by cartridge A) was assessed by presenting R1 and R6 with a sequence of brief (10-ms) stimuli [Fig. 7(c_a)] with various interstimulus intervals Δt. The sluggish impulse response obtained [Fig. 7(d)] resembles that of a second-order low-pass (LP) filter with a 10-ms dead time [124], [158]. Its time constant τ can be approximated by the observed time to peak in Fig. 7(d): $\tau \cong 50$ ms.
4) Presenting R1 and R6 with the opposite sequence of 10-ms flashes inhibited the LPTC resting discharge, and this effect was again locked to the second stimulus [Fig. 7(c_b)]. This and other experiments (see [131, Fig. 2(g)]) suggested the existence of a mirror-symmetrical EMD subunit [not shown in Fig. 7(b)] with opposite preferred direction. The latter would have a similar facilitating arm (driven by cartridge B). In this opponent subunit, facilitation would again be the rule but the facilitated signal would then act negatively on H1 via an inhibitory connection. The impulse response of this facilitating arm in charge of the opposite direction was found to show a qualitatively similar pattern: that of a second-order low-pass filter with dead time [184]. The latter result was obtained using another method of stimulation (the "telescope method" [125]) with which, instead of single photoreceptors, whole visual sampling units (comprising eight coaxial R1–R6 and R7–R8 cells; see Section IV) can be stimulated individually in the far field. One disadvantage of this approach is, however, that in the absence of a facet diaphragm [cf. Fig. 6(b) and the inset in Fig. 6(a)], the light stimuli can excite other EMDs simultaneously because the receptors' angular sensitivities are not needle shaped. The authors concluded that there may exist many EMDs driven by visual units with sampling bases up to four times the one studied here [184]. By contrast, a behavioral study carried out on *Drosophila* using drifting gratings carefully projected on the far field with the "telescope method" had inferred that EMDs are formed with the same sampling basis as the one we studied here but also, and primarily, with a sampling basis $\sqrt{3}$ smaller, along two directions oriented at $\pm 30^\circ$ to the horizontal [14], [95].
5) The dynamics of the facilitated arm [that driven by cartridge B in Fig. 7(b)] was assessed on the contrary by studying its step response. The pair of photoreceptors were exposed to a sequence of long lasting light steps [Fig. 8(a)]. Again, the first stimulus did not elicit any response but was assumed to drive the facilitating arm to a sustained value, in keeping with the impulse response shown in Fig. 7(d). The transient, quasi-exponentially decaying step response generated by the second stimulus [Fig. 8(a)] revealed the presence in the right arm of a first-order high-pass filter [158] with a time constant on the order of 100 ms (see [36, Fig. 4] for the curve fitting conducted on another recording of the step response).
6) These experiments also suggested (see also [185]) that instead of being subtracted from each other (as in the original HR model) the outputs from the two EMD subunits with opposite preferred directions may drive the LPTC directly, via excitatory and inhibitory synapses, respectively, located at nearby sites on the LPTC dendritic tree [158]. This push–pull model has been found to be consistent with the changes in resistance observed during an LPTC response to motion [186] and with the response of an LPTC recorded under polarizing and depolarizing current injections

[187], [195]. This push–pull drive has also been found to account for the nonlinearity observed in the summation of multiple EMDs on an LPTC's dendritic tree [188], obviating the need for an auxiliary feedback neuron inhibiting the EMDs' inputs [165].

All in all, these results suggested that each EMD half-detector can be said to elicit a sluggish facilitation of a high-pass-filtered signal [158]. In the preferred direction, for example [Fig. 7(b)], the high-pass-filtered signal from the right arm is picked up by the LPTC downstream, its amplitude being adjusted by the left arm sluggish dynamics. This adjustment is graded over time and contrasts with the all-or-none effect of a logic gate.

Lateral facilitation occurs gradually in a time window [10 ms $< \Delta t <$ 230 ms; Fig. 7(d)] defined by the impulse response of the lateral arm stemming from cartridge A [Fig. 7(b)]. This time window obviously constrains the angular velocity range of the EMD. Given that the inter-receptor angle between R1 and R6 is 3.6° [Fig. 3(a)], the extreme Δt values limit the angular speed range to 16°/s $< \Delta\varphi/\ \Delta t <$ 360°/s. Maximum facilitation occurs at around $\Delta t =$ 50 ms [Fig. 7(d)], corresponding to an angular speed of 72°/s [158].

From a computational viewpoint, the lateral facilitation observed here is akin to a process of "multiplication," in accordance with the HR model. From an algorithmic viewpoint, however, the two input ports of an analog multiplier do not need to play the same role, and we favored the idea that the "multiplier" depicted in Fig. 7(b) is rather a parametric control system [131], [158], much like the volume control in a radio set. Specifically, we suggested that the slow, low-pass-filtered signal [originating from the left arm, Fig. 7(b)] drives a parameter (e.g., a gain or a threshold) that sluggishly adjusts the transfer of the fast, high-pass-filtered signal from the right arm down to the LPTC [158]. Shunting inhibition, which was thought [189] to possibly account for the Barlow–Levick inhibitory model where the response to null sequences is vetoed [177], could hardly account for the facilitation observed here (see also [185]). Instead, presynaptic facilitation [190], [191] might provide the long-lasting facilitation characterized by the long-lived impulse response of the left arm [Fig. 7(b)].

How would an array of such elaborate HR detectors react to a drifting grating? For decades, the basic HR detector was described with a low-pass filter in one arm and no filter in the other arm (see, e.g., [188]). This simple scheme has been challenged over the last decades (e.g., [192]–[194]). Alternative schemes have been put forward and simulation experiments have examined the possible presence of a high-pass filter at various locations, for instance, in the two input lines to the EMD [157], [193], [194], or in the arm driven by cartridge B in Fig. 7(b) [194]. Only in the latter case did the simulation account for all the experimentally recorded responses of H1 to transiently or constantly drifting gratings [194]. The simulation also suggested that the long-known process of motion adaptation [192], [193], [196] could be accounted for by a high-pass-filter arm endowed with an *adaptive* time constant.

The low-pass–high-pass EMD scheme was implicitly adopted in a recent review [195, Fig. 4], in line with the conclusions from the analyses conducted on isolated EMDs with single photoreceptor stimulations [98], [158].

C. The Splitting of an EMD Into an ON-EMD and an OFF-EMD

The results of a crucial set of experiments using sequences of long-lasting (1000-ms) light pulses pointed to the existence of a new pattern of division of labor in the fly's visual system. Fig. 8(a) and (c) shows that only step sequences of brightness increase (ON then ON) or brightness decrease (OFF then OFF) triggered a response in H1. Sequences made of opposite contrast polarities (ON then OFF or OFF then ON) did not to trigger any responses in H1 (i.e., no « reverse-phi » apparent motion [197]): they triggered neither an increase nor a decrease in the spike frequency [Fig. 8(b) and (d)]. The main conclusion we reached (see [158, Sec. 4.7, p. 379, Fig. 16]) was that the EMD responsible for sensing motion in the preferred direction is split into two separate ON-EMD and OFF-EMD detecting sequences of light edges and dark edges, respectively, both EMDs contributing to the overall response [Fig. 8(e)]. The four-quadrant multiplier in the HR scheme is, therefore, split into a pair of twin multipliers [Fig. 8(e)]. The twin EMD subunits presented here in the case of the preferred direction [Fig. 8(e)] both drive H1 with the same (positive) polarity (and not with opposite polarities, as suggested by other authors [87]).

The two transient step responses measured in H1 [Fig. 8(a) and (c)], which are locked to the onset of the second stimulus in the sequence, approximate the step response of a high-pass filter of 100 ms time constant, and are reminiscent of the ON and OFF transient components of L1 and L2 step responses [119], [120], [139], [cf. Fig. 2(c), bottom traces]. This suggests that the ON- and OFF-responses of H1 may derive more or less directly from the L1 and L2 transient components which, after adequate signal inversion and half-wave rectification, may be "flushed down" separately to H1 through their respective multiplier/parametric control [see Fig. 8(e), bottom signals].

Doubling the pathway may, at first sight, appear as a profligate strategy of the nervous system, but the split EMD is of interest in many respects.

1) It alleviates the correspondence problem in the motion detector [200] by automatically bringing into correspondence only edges of the

same polarity (increases or decreases in brightness) [158].

2) It increases the refresh rate in the motion estimates since both the leading edge and the trailing edge of a (dark or light) moving object contribute an input to the LPTC [158].
3) It allows the two neurons driving the LPTC [Fig. 8(e)] to operate with a low level of activity at rest (which is relevant to the energy budget [201]), and to use their full dynamic range for signaling the motion of a light edge and dark edge, respectively. A similar argument has long been put forward in connection with the ON- and OFF-pathways of the vertebrates' visual systems [202], [203].
4) It alleviates the biophysical problem raised by the implementation of the four-quadrant multiplier required in the HR model [10]. Each EMD subunit now requires two parallel multipliers for each direction of motion, but each multiplier can be obtained more simply. Adequate signal inversion and half-wave rectification can make the signals at the two ports of each "multiplier" unipolar. Each multiplier, therefore, needs to be a simple one-quadrant multiplier. We have obtained evidence for half-wave rectification in the high-pass arms [204], and recent calcium recordings from L2 terminals in the medulla have indicated how this process may take place, at least in the OFF-pathway [206].

D. Toward the Cellular Implementation of an EMD

Two parallel streams have been described in the fruitfly *Drosophila*, which lead from lamina cartridges down to single columns in the lobula plate [110], [112], [167], [181]. Several recent studies based on electrophysiological recordings and behavioral tests combined with genetic methods have shed new light on the split pathways involved in flies' visual motion perception [199], [207]–[209]. In particular, the results obtained (using much coarser types of optical stimulation such as drifting gratings or sequentially flashed bright or dark slits) while genetically silencing one of the two large monopolar cells L1 and L2 in the lamina of the fruitfly have suggested that the ON-EMD is driven by L1 and the OFF-EMD by L2 [Fig. 8(e), top colored letters]. This exquisite refinement at the cellular level [107], [199] confirms the finding we made on the inner processing structure of an EMD, which was shown to be split into an ON-EMD and an OFF-EMD part [158].

LPTCs have long been thought to be driven by the columnar cells T4 and T5, which take input in the medulla (e.g., [110], [112], [167], [181], and [210]–[212]). This view has recently been confirmed by elegant experiments again using genetic tools. Blocking both T4 and T5 cells abolished the electrical response of (a subset of) LPTCs [213], and selective blocking of either T4 or T5 cells compromised not only the LPTCs' responses but also the optomotor response of tethered walking flies to moving ON- and OFF-edges, respectively [108]. Moreover, direct optical recordings of calcium signals performed on both the T-cells' axons and their minute terminals in the large dendritic tree of an LPTC have shown that both T4 and T5 terminals are strongly direction selective [108]. T4 and T5 cells may, therefore, jointly constitute the two long sought-for EMD subunits [Fig. 8(e), bottom colored letters] which transmit to the LPTCs the signals corresponding to moving bright edges and dark edges, respectively [108]. Finally, part of the synaptic links between the lamina (L1 and L2) cells and the input (T4 and T5) cells to the LPTCs, which had been suggested earlier [167], have recently been confirmed in a remarkable and painstaking connectome analysis. Two neighboring L1 neurons may drive one T4 cell via two distinct medulla neurons, Mi1 and Tm3, that may be considered as the two arms of an EMD subunit [130]. The medullary connections between L2 and T5 possibly involve Tm1 [130], [167] but remain to be firmly established.

In fact, no less than four T4 cells and four T5 cells per column have been found to occur in *Drosophila* [112]. This could make for eight different EMD subunits (four ON- and four OFF-subunits). This is precisely what the recent experiments suggested [108], and most interestingly, the two subpopulations of four EMDs were found to have preferred directions corresponding to the four cardinal directions of motion: down, up, left, and right, and to project most appropriately to the four directionality layers of the LP [see Fig. 5(b), inset]. In each of these four directions of motion, one T4 cell delivers the ON-EMD input and one T5 cell delivers the OFF-EMD input to the dendrites of the wide-field LPTCs [107], [108]. The latter findings are particularly noteworthy since they constitute the very first evidence in favor of the existence of strongly directional EMD subunits presynaptic to an LPTC [107], [108]. This holds at least for the case of the EMDs responsible for the four preferred directions ($\downarrow, \uparrow$ and $\leftarrow, \rightarrow$). The mystery still remains to be solved as to which neurons make up the mirror-symmetric EMD subunits exerting inhibitory effects in the four antipreferred directions ($\uparrow, \downarrow$ and $\rightarrow, \leftarrow$).

The question arises as to whether the neurons stemming from cartridge A [Fig. 8(e)], which drive the two facilitating arms, can simply be assigned to another pair of L1 and L2 cells, as recently suggested (see [108, Suppl. Fig. 2]). This seems to be unlikely because it would be incompatible with the dynamics of these lateral arms, which produce a long-lasting impulse response corresponding to a low-pass filter [Fig. 7(d)] and accordingly a sustained step response which in no way resembles the (transient) step response observed in both L1 and L2 [Fig. 2(c), bottom recordings]. Besides, the data in [106], obtained with coarser optical stimuli, seem to contradict the assumption that only information about brightness changes is passed on to the motion detection circuitry (see

also [209]). And it has long been held that at least one of the two inputs of an EMD must deliver a tonic signal [214], which neither L1 nor L2 can afford. Therefore, it remains to be established which lamina cell(s) may provide input(s) to the two facilitating arms. The only known tonic efferent neuron is the (hitherto unidentified) "Arnett's sustaining unit" detected in the outer chiasm connecting the lamina to the medulla [215], [216].

E. Summary

The housefly's compound eye samples the world via 3000 "visual sampling units," each of which comprises eight photoreceptor cells pointing in the same direction and forming both color channels (cells R7 and R8) and a coaxial high-sensitivity channel (cells R1–R6) subserving motion detection in particular. The lobula plate contains about 50 directionally selective motion-sensitive neurons. These wide-field LPTCs take input from hundreds of EMDs and act as OF sensors involved in head stabilization and visual guidance. By recording the electrical activity from one of these neurons and applying sequential illumination to two single photoreceptors behind a single facet, the inner processing structure of an isolated EMD was studied with a high resolution. The resulting EMD model consists of an elaborate HR detector, each subunit of which contains a second-order low-pass filter in one arm and a first-order high-pass filter in the other arm [Fig. 7(b)]. The signal delivered by the low-pass arm does not show up in the EMD response, but covertly facilitates the passage of the high-pass-filtered signal from the second arm down to the wide-field LPTC. Single-cell stimulation studies further showed that each of the two mirror-symmeric EMD subunits is split into two parallel ON- and OFF-pathways [Fig. 8(e)]: one detects the motion of bright edges, and the other one captures the motion of dark edges separately. Recent neurogenetic, optogenetic, and connectomic studies on the fruitfly have provided neuroanatomical support for the existence of this split pathway, and identified part of the neuronal chain from the EMD inputs in the lamina down to the EMD outputs on the dendrites of the LPTCs.

VI. FROM NATURAL TO ARTIFICIAL OPTIC FLOW SENSORS

Sections VI–X describe briefly some of the bio-inspired sensors and robots developed at our laboratory over the last 30 years. The reader is referred to the original papers for a more detailed description.

In the mid-1980s, inspired by the EMD processing structure we discovered in flies [Figs. 7(b) and 8(e)] we built electro-optic EMDs, the output of which increased monotonically with the angular velocity of a nearby moving edge [217]–[219]. This involved determining the time of flight Δt taken by an edge to move across the interreceptor angle $\Delta\varphi$ of two photodiodes Ph1 and Ph2 [Fig. 9(a)].

The photodiodes were placed near the focal plane of a lens with an appropriate defocus giving Gaussian-shaped FOVs, as occurs in the FOV of the fly's photoreceptors [cf., Fig. 3(a)]. After this spatial filtering step, the two photodiode signals were temporally bandpass filtered [Fig. 9(b)]. Their step response resembled that of the large monopolar cells L1 and L2 present in the fly lamina [cf., Fig. 2(c), bottom panel]. The next processing step consisted in performing hysteresis thresholding and generating a unit pulse in both channels [Fig. 9(b)]. In the EMD version we built for the Robot Fly [36], [219], the unit pulse from the second channel sampled a long-lived decaying exponential function generated by the first channel via a nonlinear circuit called the minimum detector [Fig. 9(b)]. This operator, which was implemented very simply with just two diodes and one resistor, performed one-quadrant multiplication of the (constant and positive) unit pulse [the red pulse in Fig. 9(b)] with the (always positive) amplitude of the decaying exponential function at time Δt. A short Δt therefore gave a high voltage output and *vice versa*. The output signal was a monotonic function of the local OF $\Delta\varphi/\Delta t$, and the thresholding step made the output voltage relatively invariant to contrast in the 0.15–0.75 range [36], [219]. Neuromorphic EMDs of this kind are also able to respond to natural moving panoramas [220].

This type of EMD cannot be said to be a correlator, and corresponds rather to a feature-matching scheme [200], where a given feature [here, a passing edge: Fig. 9(a) and (b)] is extracted and tracked with time. A very similar principle for designing a velocity sensor was developed a decade later at the California Institute of Technology (Caltech, Pasadena, CA, USA) and called the "facilitate-and-sample" velocity sensor [221], [222]. Another analog VLSI chip based on our original time-of-flight scheme was developed yet another decade later and called the "time-to-travel" scheme [223].

In the analog circuit [Fig. 9(c)] designed in 1989 for the Robot Fly, we also applied our latest findings on flies in terms of the splitting of the EMD into two separate and independent ON-EMD and OFF-EMD responsible for detecting the motion of a bright and dark edge, respectively [158], [204], [225]. The circuit in charge of each motion direction was therefore doubled, and the necessary signal inversions and half-wave rectifications were included in each subunit, giving a total number of four EMD subunits on each miniature board (two in the preferred direction, and two in the antipreferred direction) [Fig. 9(c)]. We also made each EMD subunit immune to synchronous flicker, as found to occur in the fly [see Fig. 6(c_c)].

Over the years, we have implemented this EMD using either discrete analog components [Fig. 9(c)], a field-programmable analog array (FPAA by Anadigm) [51], or hybrid techniques [e.g., Fig. 9(d)] involving the use of tiny microcontrolers [229]. The smallest hybrid circuit developed so far [Fig. 9(d)] weighs only 0.2 g [226]. Using the

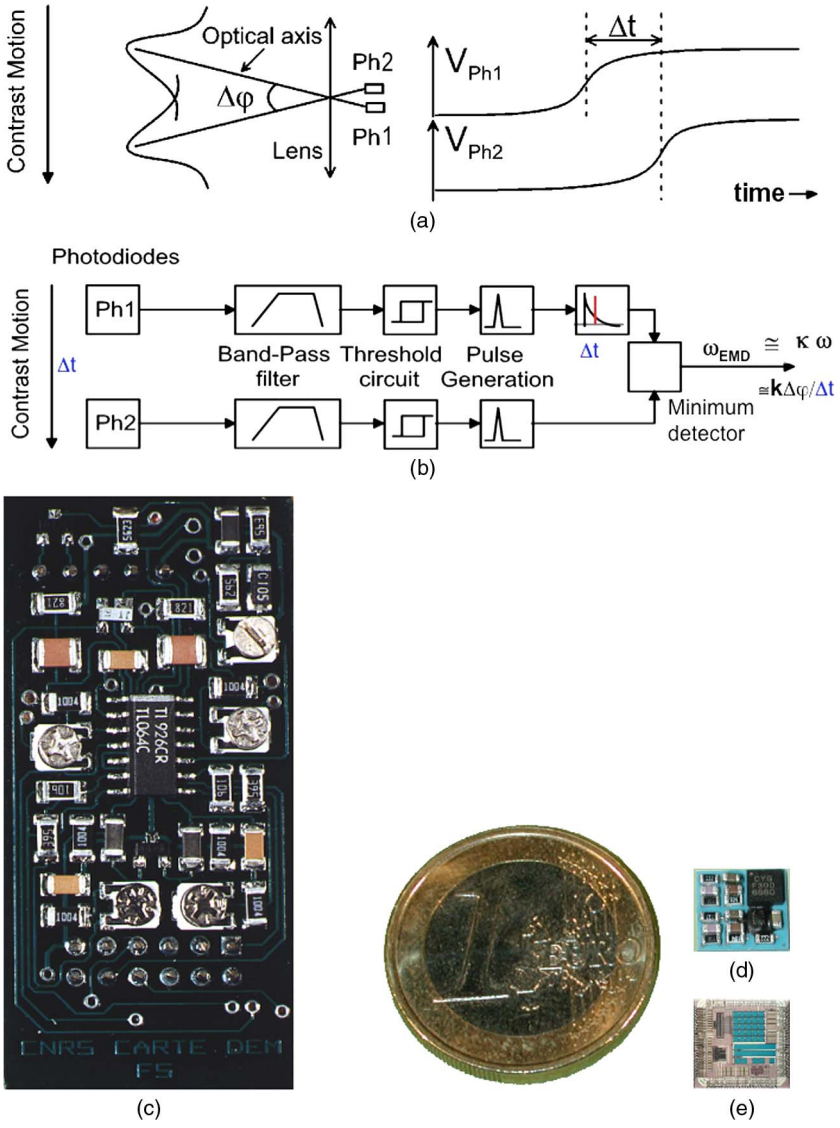

Fig. 9. *Principle and construction of an electro-optic EMD inspired by the functional diagram of the fly's EMD analyzed by stimulating single photoreceptors [cf Figs. 7(b) and 8(e)]. (a) Motion of a contrasting edge occurring in the FOV of a pair of photodiodes Ph1 and Ph2 (interreceptor angle $\Delta\varphi$) induces a time lag Δt in their electrical responses [51]. (b) Principle of the EMD: after low-pass (spatial) filtering and bandpass (temporal) filtering steps, the signals from Ph1 and Ph2 were thresholded, generating a unit pulse in both pathways. The pulse from pathway (2) was used to sample the decaying exponential function generated by the pulse from pathway (1) by means of a minimum detector, the output of which therefore increased monotonically with the local OF $\omega = \Delta\varphi/\Delta t$ (adapted from [224] and [46]). (c) Purely analog version of a 5-g electro-optic EMD developed in 1989 [219], [224]. Each board housed two EMDs (one specialized in each direction) each of which was split into an ON-EMD and an OFF-EMD, as occurs in flies [cf., Fig. 8(e)]. (d) The 0.2-g version developed in 2007 (involving a tiny microcontroller [229]) and constructed using low-temperature cofired ceramic technology (LTCC) [226]. (e) Analog VLSI array comprising 25 adaptive photoreceptors driving EMDs based on a miniature 0.4-g FPGA [220], [228].*

field-programmable gate array (FPGA) technology, we have shown that up to 245 EMDs could be implemented on a small (12 mm × 12 mm) FPGA [230]. We have also combined a VLSI chip consisting of 25 photodetectors [Fig. 9(e)], each equipped with an adaptive photoreceptor front end [227], with a miniature FPGA [220], [228]. All the proof-of-concept robots described below were based on one or other version of these fly-inspired OF sensors.

VII. THE ROBOT FLY

In the mid-1980s, we took up the challenge of designing a robot capable of guiding itself through a complex environment on the basis of optic flow cues. The Robot Fly was based on the process observed in insects whereby sensory signals are rapidly and efficiently transformed into appropriate motor commands (see, e.g., [231]). This robot

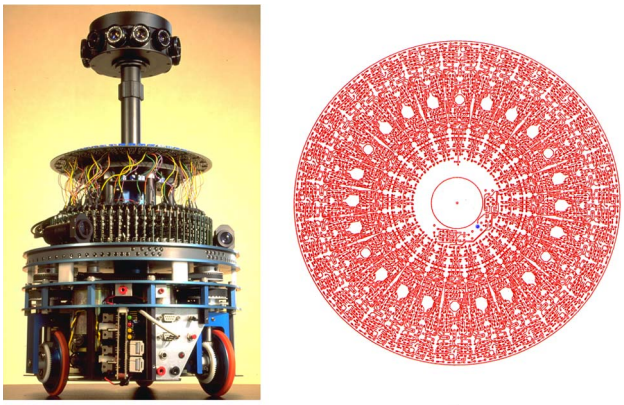

(a) (b)

Fig. 10. *(a) The "Robot-mouche" (in English: the "Robot Fly") developed in 1991, equipped with a panoramic compound eye (visible here at half-height) and an omnidirectional target seeker (at the top), all mounted on a synchro-drive tricycle (Real World Interface). The robot reacts to the OF generated by its own locomotion. Behind the compound eye is an array of 114 EMDs [cf., Fig. 9(c)] equipped with PIN photodetectors operating in the logarithmic mode. (b) Routing diagram of one face of the printed circuit board (PCB), implementing the anticollision algorithm in a fully parallel mode. This six-layered PCB has 210 parallel inputs (114 EMD inputs plus 96 inputs from the target seeker) and a single meaningful output (the blue point near the center of the pattern) giving (in volts) the next tack to be set to reach the target while avoiding obstacles. This side and the reverse side of the PCB are both covered with thousands of analog devices of four kinds (resistors, capacitors, diodes, and operational amplifiers). This neuromorphic board includes both a resistive network [88] and a diode network [224] fusing the signals stemming from the compound eye and the target seeker. The layout is reminiscent of the neural architecture of the visual areas present in animal brains. The rose-window-like pattern results from the presence of many repeat units and their retinotopic projections (originally published in [36] and [233].*

viewed the world through a horizontal ring of facets, such as those shown at half-height in Fig. 10(a). Behind the facet array was an array of PIN photodiodes operating in the logarithmic mode. Any two adjacent facets drove a fly-inspired EMD [of the type shown in Fig. 9(c)], and there were 114 EMDs in all sensing the OF field in the horizontal FOV. These EMDs were used to sense the translatory OF generated by the robot's own locomotion and to use these data immediately in a purely reflexive algorithm. The robot did not rely on a global representation of its environment to steer its way to the target.

The 50-cm high Robot Fly we produced in 1991 [Fig. 10(a)] was the first completely autonomous OF-based robot able to avoid contrasting obstacles encountered on its path while traveling toward a target at a relatively high speed (50 cm/s) [36], [224], [232], [233]. The Robot Fly was directly based on ethological findings on real-life flies, whose flight trajectories have been found to consist mainly of straight flight episodes (lasting 50–200 ms) interspersed with rapid turns known as saccades [20], [21], [96], [234], [235], [236]. A straight flight sequence performed at speed V near an obstacle located at distance D and azimuth φ with respect to the heading direction generates in the robot's eye a translational OF ω [rad/s] which can be expressed as follows [237], [238]:

$$\omega = \frac{(V.\sin\varphi)}{D}. \tag{1}$$

This means that if a robot (or an animal) is able to measure ω, it will be able to gauge the distance D to the obstacle, as long as it knows its own speed V. The Robot Fly proceeded by performing a series of purely translational steps ΔL (length 10 cm; duration 200 ms) at a speed set at $V = 50$ cm/s via the wheel encoders. The various local OFs measured along a given ΔL were buffered up to the end of the step. By the end of each step, the panoramic EMD array had therefore drawn up a map of the local obstacles, which was expressed in polar coordinates in the robot's reference frame. Any contrasting obstacle detected caused the translatory phase to be interrupted by a fast, saccade-like rotation, during which vision was inhibited (as the result of a "saccadic suppression" process (cf., [239]) to prevent the adverse effects of rotational OF. In addition, we provided this compound eye with a resolution gradient causing the interreceptor angle $\Delta\varphi$ to increase according to a sine law as a function of the eccentricity φ. This nonuniform sampling procedure, which is reminiscent of the smooth resolution gradient existing across the fly's eye as observed in the far field with a telescope [125], "compensated" for the sine law inherent to the translational OF field [see (1)]. Once embedded in the anatomical structure of the eye, this resolution gradient ensured that any contrasting feature would be detected regardless of its azimuthal location if, during a robot's translation by ΔL, this feature entered the robot's "circle of vision," the radius Rv of which was proportional to ΔL

$$Rv = k\Delta l. \tag{2}$$

Any contrasting feature which was more distant than Rv was automatically "filtered out" (i.e., not detected) because it would not have crossed the two visual axes of an EMD during the ΔL translational step. An additional advantage of this nonuniform sampling process is that all the underlying EMDs [Fig. 9(c)] could be built uniformly with the same time constants as their neighbors. This feature greatly simplifies not only the engineering of a robot, but also in a similar way the genetic specification of an animal nervous system. Part of the "intelligence" of the visual system was therefore embedded right in its structure (cf., [240]).

No stop occurred at the end of a translation step if no steering command was issued, i.e., if no obstacle had been detected by the EMD array. The elementary translation steps were seamlessly connected due to the high processing speed of the parallel, analog mode used. The robot took a rather jerky trajectory, skirting any obstacles encountered before reaching the target.

The Robot Fly provided physical evidence that a mobile agent equipped with low acuity (having only 116 pixels) but extremely widefield vision can avoid obstacles at a relatively high speed (50 cm/s) by reacting to the translational OF generated by its own locomotion.

Further developments tested in computer simulations have enabled a robot of this kind not only to drive around obstacles at a high speed but also to automatically adjust its speed to the density of the looming obstacles. This ability emerges automatically if, instead of imposing on the robot constant ΔL translation bouts as described above, one imposes constant Δt translation times [241]. During any one Δt, the robot will cover a distance ΔL proportional to its current speed V. From (2) and (1), one can calculate the new radius Rv of the circle of vision

$$Rv = k.\Delta l = k.V.\Delta t = k'.V. \tag{3}$$

The radius of vision Rv now increases in proportion to the speed, which makes it possible for the robot to see (and, therefore, to avoid) obstacles within a range that increases suitably with the speed of travel. This is indeed very suitable behavior for robots, animals, and humans. Simulations based on this principle have shown the robot making a detour around a dense forest (represented by a large set of trees forming the obstacles), then automatically accelerating in a clearing and automatically braking before traversing the second, less dense forest (see [241, Fig. 3]).

VIII. FANIA, OCTAVE, AND LORA

Although the first few steps made by the Robot Fly at our lab were a "giant leap" for us, we soon admitted that it was cheating because it was "aware" of its own speed (via the tachometer coupled to one of its wheels). By contrast, insects and birds are able to fly without any connections with the ground from which they might estimate their groundspeed. How then do these aerial creatures measure their groundspeed and groundheight and solve the control problems involved in performing visually guided short range navigation? In the spirit of the Wright brothers I knew that as a onetime bicycle maker (Fig. 1), I would end up by building some kind of a flying machine. The first experimental simulations we run showed that the same motion detection principles as those used in the Robot Fly can be used to guide a flying agent, have it follow a rough terrain, and land automatically on command [23]. The principle was first tested onboard FANIA, a miniature experimental helicopter system equipped with a variable-pitch rotor and a low-resolution eye composed of 20 pixels covering the frontal–ventral region and driving 19 EMDs [23]. FANIA was attached to a light, pantographic, and counterbalanced beam that kept it stable on the vertical plane. This 0.8-kg sighted rotorcraft was made to take off by increasing the rotor's collective pitch, and to pitch forward by remotely orienting the servo–vane located in the propeller wake. FANIA then achieved autonomous terrain avoidance by automatically adjusting the collective pitch as a function of the fused signals transmitted by the EMD array. Experimental tests showed that FANIA was able to consistently jump over the 30° slanted part of its circular track (see [23, Fig. 8]).

Behavioral observations published in the 1950s suggested the hypothesis that locusts may have a "preferred ventral OF" and that they may navigate on this basis [18]. Although this hypothesis has been repeatedly confirmed in the case of various insects during the last 30 years [243], it does not tell us exactly how the insects proceed. The reason is that the ventral OF ω is a ratio [as shown in Fig. 11(a)]

$$\omega = \frac{V_x}{h}. \tag{4}$$

A "preferred ventral OF" ω could, therefore, be obtained by an infinitely large number of possible combinations of groundspeeds V_x and groundheights h. In attempting to formalize the problem, we ended up by designing an autopilot called OF-based Control sysTem for Aerial VEhicles (OCTAVE) involving a feedback loop called the OF regulator [Fig. 11(c)], which acts upon the lift so as to maintain the downward OF ω constant and equal to a set point [ω_{set} in Fig. 11(c)] [51], [243].

We then devised an elementary proof-of-concept microhelicopter equipped with this autopilot [51]. When tested on a flight mill, this 100-g sighted rotorcraft [Fig. 12(a)] was found to be able to perform challenging maneuvers such as terrain following at various speeds (from 1 to 3 m/s), automatic takeoff, and automatic landing, while reacting smartly to wind perturbations [244]. In this system, a single ventral EMD continuously measured the OF ω_{meas} in the downward direction and compared it with the OF set point ω_{set} [Fig. 11(c)]. The error signal $\varepsilon = \omega_{\text{meas}} - \omega_{\text{set}}$ controlled the robot's lift, and hence its groundheight, via the surge dynamics so as to maintain the perceived OF at the OF set point. This occurred whatever the robot's groundspeed V_x, and whatever disturbances were encountered which were liable to affect the groundspeed and groundheight.

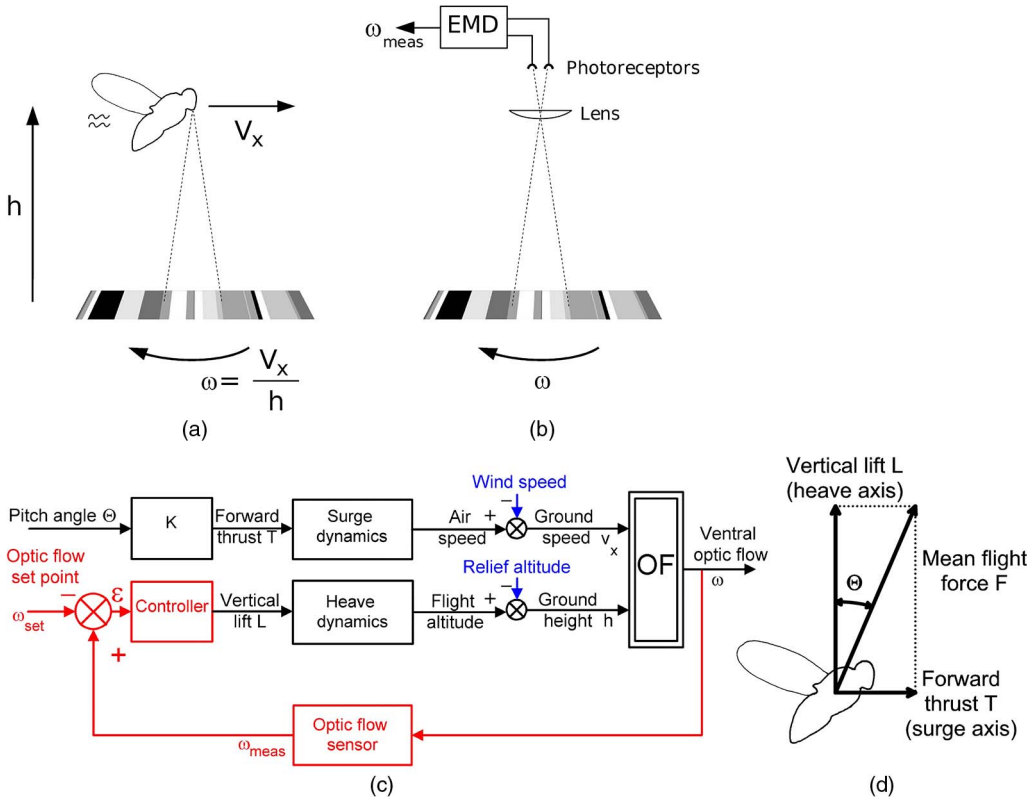

Fig. 11. ***(a) Definition of the ventral OF ω experienced by an insect, a pilot, or a robot traveling in a straight line above the ground. (b) EMD of the type shown in Fig. 9 is able to measure the ventral OF, i.e., the relative angular speed ω [rad/s] at which any contrasting feature on the ground seems to move backward under the flying agent [243]. (c) The OF regulator OCTAVE (red feedback loop) is a nonlinear feedback control system that essentially controls the vertical lift and hence the groundheight, so as to maintain the measured ventral OF ω_{meas} constant and equal to the OF set point ω_{set} [50]. The controller includes proportional and derivative (PD) functions, which ensures closed-loop stability in the groundspeed range of 0–3 m/s. (d) Flies pitch forward slightly to increase their forward thrust, and hence their airspeed. Any change in the mean flight force F vector mainly affects the lift L as long as $\Theta < 10^\circ$ [243].***

Four particularly noteworthy results were obtained in these studies [51], [243]–[245].

1) The OCTAVE autopilot automatically brought the robot to an altitude that increased suitably with the flying speed. Clearance of the ground increased in proportion to the groundspeed and depended on the value of ω_{set} [51].
2) Risky maneuvers such as automatic takeoff, ground avoidance, terrain following, suitable reactions to wind and automatic landing [Fig. 12(-b_a)] were all performed thanks to a single feedback control loop [Fig. 11(c)] [243], [244].
3) Landing on a flat surface occurred automatically at a constant slope α which depended on both the OF set point ω_{set} and the robot's surge time constant τ [243]

$$\alpha = \arctan\left(\frac{1}{(\tau.\omega_{\text{set}})}\right). \quad (5)$$

4) These challenging maneuvers were all performed without the robot being given any explicit information about the absolute altitude, local groundheight, groundspeed, descent speed, or windspeed [244], [245]. Unlike the Robot Fly, OCTAVE did not measure any distances and was not "aware" of its groundspeed either.

This bio-inspired autopilot, therefore, differs strikingly from classical man-designed autopilots, which often need a large number of costly and bulky airborne metric sensors [such as a barometric altimeter, a radio-altimeter, a Doppler radar, a laser range finder, a forward looking infrared (FLIR) system, a Global Positioning System (GPS), and a variometer] to hold the aircraft's altitude and groundspeed, as well as costly off-board instrumentation [such as instrument landing systems (ILSs)] to be able to achieve automatic landing at a constant descent angle. OCTAVE's main objective is to keep a safe clearance from the ground at all speeds and not to hold the altitude or groundspeed. OCTAVE does not even bother about state variables such as the groundspeed and groundheight. And

(a)

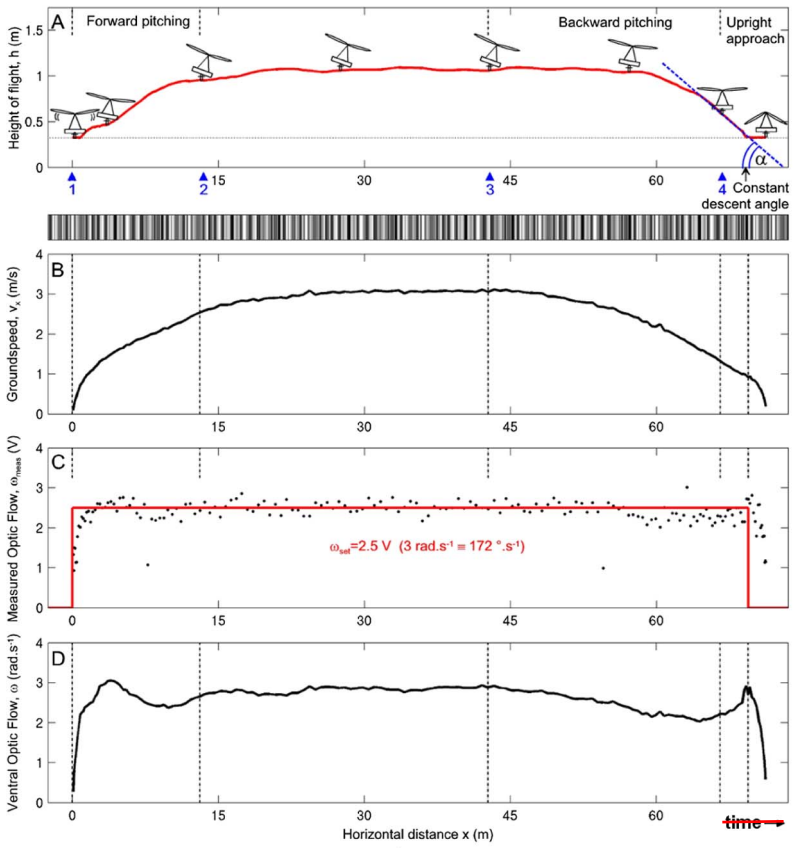

(b)

Fig. 12. *(a) The 100-g microhelicopter (MH) equipped with a single ventral OF sensor [EMD, Figs. 9 and 11(b)], and the OF regulator shown in Fig. 11(c). The single EMD sensor, always pointing vertically downward, was able to detect relative angular speeds, ω occurring within the range of 40–400°/s, whatever the contrast m (down to $m = 0.04$) [243]. The tethered MH could be remotely pitched forward by a small angle Θ while keeping its roll attitude. It was able to take off and circle at speeds of up to 3 m/s and heights of up to 3 m over a large ring-shaped track (outside diameter: 4.5 m) covered with stripes showing a random width and a random contrast, as in Fig. 11(a). The flight mill was equipped with ground-truth azimuthal and elevation sensors with which the position and speed of the MH were monitored accurately in real time. (b) Flight variables monitored during a 70-m flight of the MH over the randomly textured pattern (shown below the flight path in (b_a), including takeoff, level flight, and landing. (b_a) Flight path consisting of about six laps on the flat test arena. (b_b) Monitored groundspeed V_x. (b_c) Output ω_{meas} of the OF sensor, which can be seen to remain virtually constant (3 rad/s) throughout the flight path thanks to the optic flow regulation loop. (b_d) Actual OF calculated as the actual V_x/h ratio. (Photograph in (a) courtesy of M. Vrignaud; (b) is taken from [243].)*

since the OF regulator constantly strives to maintain the OF near the OF set point, the resulting behavioral performance of the robot can be said to make the OF sensor target the most appropriate operating point, which results in modest requirements in terms of the EMD's dynamic range [243]. This study was recently extended to include terrain following and landing in nonstationary environments such as laterally drifting and vertically oscillating platforms [242].

On similar lines, we established that a fully actuated miniature hovercraft equipped with a dual OF regulator can achieve both lateral obstacle avoidance and cruise control while flying along a corridor [246]. In the experimental simulations we performed, the OF-based autopilot called the lateral OF regulation autopilot (LORA) automatically adjusted both the hovercraft's groundspeed and its clearance from the walls without having to make any groundspeed or distance measurements. LORA, equipped with the eponymous autopilot, navigates at sight on the basis of two parameters, namely the set points of two intertwined OF regulators: a sideways OF set point and a forward OF set point [60], [247]. These two parameters alone suffice to constrain the vehicle's behavior in a straight or tapered corridor [247], resulting not only in wall-centering performances resembling those of honeybees [248] but also in wall-following performances, again resembling those of honeybees [249].

In comparison with the Robot Fly [Fig. 10(a)] which assessed the distance D from obstacles according to (1) (where φ and V were given and ω was measured with its EMDs), the aerial robots FANIA, OCTAVE, and LORA are major improvements as they are able to fly around at relatively high groundspeeds without having to measure any groundspeeds or the distance from the substrates (the ground in the case of FANIA and OCTAVE, and the lateral walls in the case of LORA).

These studies suggest that similar OF regulators may well be implemented onboard insects, which probably do not assess their groundspeed or the distance from the surroundings (the ground, lateral objects, etc.), because they do not need to do so. As a matter of fact, the OF regulator concept and the robots' performances were found to account for a series of puzzling, seemingly unconnected flying abilities observed during the last 70 years in various insect species (details in [243]): for example, the fact that insects descend in a headwind [18], [250], land on a flat surface with a constant slope [251], and sometimes drown when flying over mirror-smooth water [252]. The LORA autopilot scheme [246] and the behavior it generates [60], [247] account remarkably well for the flight patterns shown by honeybees flying along a stationary or nonstationary corridor [253], and even along a tapered corridor [253]. These autopilots seem to mimic an essential aspect of insects' and birds' visually guided flight, and suggest novel generic principles for the automatic visual guidance and landing of MAVs and MSVs—principles which do without conventional, bulky, costly avionic sensors.

IX. SCANIA AND OSCAR 1

We have addressed the intriguing retinal microscanning process that we discovered in the fly's compound eye (Section IV and Fig. 4), again by using a biorobotic approach that included computer simulations followed by the construction of visual sensors and robots. Our attempts to solve this puzzling problem actually inspired four biorobotic projects, three of which were based on the assumption that the microscanning process at work in flies has something to do with motion detection.

The first project resulted in a 0.7-kg wheeled cyclopean robot SCANIA, which was able to move about in a square arena under its own visual control, avoiding the four contrasting walls despite the very low resolution of its eye (only 24 pixels covering a 60° frontal FOV) [44], [254]. This surprising ability was due to the fly-inspired symmetrical anterograde retinal microscanning process (see [180, Fig. 5(a) and (b)]) occurring at a constant speed (a periodic sawtooth waveform with a frequency of 5 Hz), which enabled the robot to detect any obstacles located at an azimuth φ close to the heading direction [i.e., near the frontal pole of the OF field, where $\varphi \rightarrow 0$ in (1)]. What the periodic microscanning movements actually do is to periodically add a given amount of rotational OF ω_r to the (very small) translational OF ω_t generated by frontal obstacles. The resulting OF is then measured by an EMD [of the kind shown in Fig. 9(c)]. Since the amount of optic flow added ω_r is known onboard, its value can be subsequently subtracted from the measured OF ω_{meas} to give the purely translational OF $\omega_t = \omega_{\text{meas}} - \omega_r$, which is the only OF component depending on the distance D (scaled by the speed of travel V) [see (1)]. The linear microscanning process was shown to greatly improve the detectability of small translational OFs that would otherwise have remained subliminal [44], [180], [254]. With hindsight, this ability suggests that the fly may also use its retinal microscanner for the same purpose, thus alleviating the problems caused by both the frontal pole of the OF field and the relatively coarse spatial sampling ($\Delta\varphi \cong 2°$) of its compound eyes.

The second project that we carried out on the basis of the fly's retinal microscanner yielded a novel optronic sensor called the Optical Scanning sensor for the Control of Aerial Robots (OSCAR) [255], [256], and a small eponymous aerial robot OSCAR I [46] equipped with this kind of sensor [Fig. 13(a)].

Briefly, in the latest version of the OSCAR sensor [256], retinal microscanning was performed on an elementary retina placed behind a lenslet and consisting of two photodiodes mounted at the tip of a high bandwidth piezoelectric bender. The latter was driven at 10 Hz, resulting in a periodic angular scanning of the environment by each of the two photoreceptors [cf., Fig. 4(c)]. During the first half (50-ms duration) of the scan cycle, the photodiodes scanned their (small) FOV at an angular speed $\omega = d\varphi/dt$ [cf., Fig. 4(c)] that was made to decay

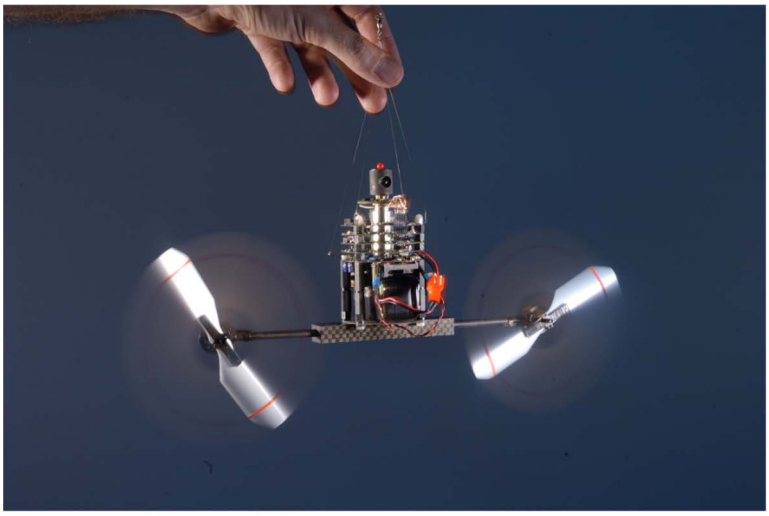

(a)

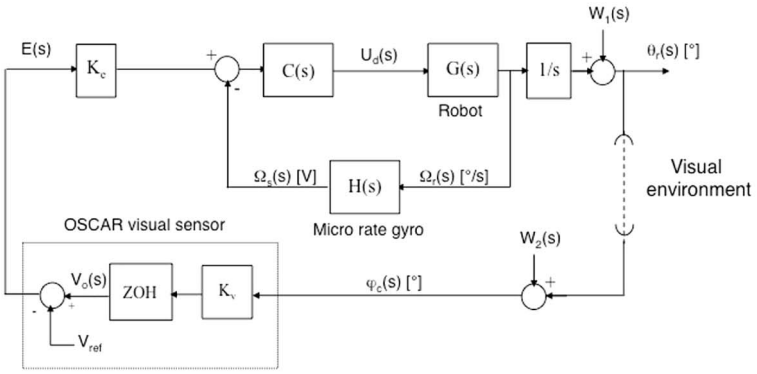

(b)

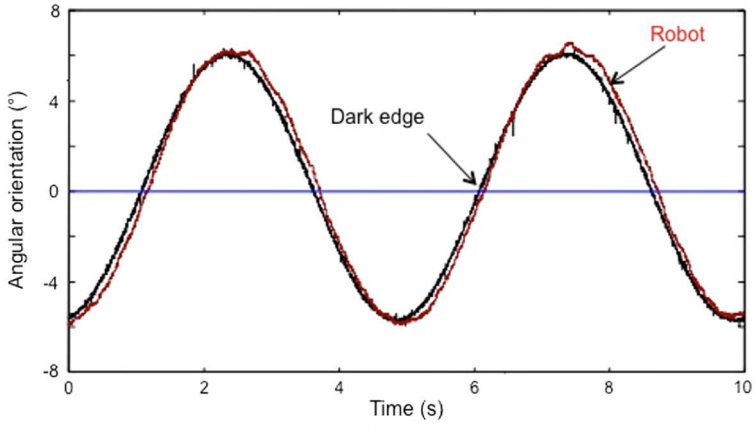

(c)

Fig. 13. *(a) OSCAR I is a tethered twin-engine aerial robot (0.1-kg mass) equipped with a microscanning eye inspired by that used by flies on the wing (cf., Fig. 4). Here, the elementary eye (visible at the top of the figure) was composed of a lens (5-mm diameter, 8.5-mm focal length) and two matched photoreceptors driving an EMD of the type shown in Fig. 9. The eye was mounted on the axis of a micromotor generating a microscanning motion with a frequency of 10 Hz. During the first half-period the speed varies according to a decaying exponential function and during the return phase the speed is constant. OSCAR is able to detect and track an edge or a bar moving at a speed of up to 30°/s [259]. Its lasting power is up to one hour. (b) Block diagram of the OSCAR's closed-loop control system, which includes the OSCAR scanning eye in the outer loop and a micro rate gyro in the inner loop. The sensor's output signal is kept constant by a zero-order hold (ZOH) up to the end of each scan period (T = 100 ms). W1(s) is an output perturbation induced, for example, by blowing on one propeller. W2(s) is the optical perturbation resulting from the target being displaced in the FOV. (c) Red curve: sinewave movement of a dark edge with a low contrast (m = 0.2) displaced sinusoidally at a frequency of 0.2 Hz in a frontal plane, 1 m from the eye. Accurate monitoring of OSCAR's heading orientation was obtained by mounting the robot on the axis of a miniature low-friction, low-inertia resolver [cf., Fig. 14(a)]. (Photograph in (a) courtesy of H. Raguet; (b) and (c) are taken from [46].)*

exponentially with time. In the second half, the photodiodes returned to their original position at a constant speed. The effect of the scan phase at a variable speed amounted to coding the relative angular position of an edge occurring in the sensor's FOV in terms of an angular speed, which was then decoded by an EMD. This resulted in the highly accurate OSCAR sensor: an optical position sensing device, the output of which was quasi-proportional to the angular position between the sensor's axis and the target (an edge or a bar), and largely invariant to distance and contrast [256].

OSCAR is able to detect an edge at a distance of up to 2.5 m, even at low contrast levels ($m = 0.1$), and a thin contrasting bar which is about eightfold finer than the pixel angular pitch [256]. In addition, OSCAR was shown to be able to locate a contrasting edge with a resolution which is 70-fold greater than its static resolution, i.e., the resolution in the absence of scanning (see [256, Fig. 13]). These results show that the OSCAR visual sensor is endowed with two kinds of hyperacuity [257]: detection hyperacuity and location hyperacuity [256]. Due to these unusual performances obtained at low cost, we have suggested that a sensor with a wider FOV obtained using an array of adjacent OSCAR sensors could be suitable for application to power line detection onboard full-scale helicopters [258].

It should be noted that the high performances of both SCANIA and OSCAR sensors ultimately result from an active visual process involving continuous retinal micromovements which transform steady photoreceptor signals into continuous temporal signals (see also [156]). And it is ironic that hyperacuity can result from the association of retinal micromovements with Gaussian blur [256] [259], given that both features are badly avoided in conventional digital imaging as they smear the image. The hyperacuity brought about by such spatio–temporal transformations has also been discussed in the context of human fixational eye movements [205].

OSCAR I [Fig. 13(a)] is a tethered twin-engine aerial robot (100-g mass) equipped with an OSCAR sensor. It was attached via a swivel to a thin, 2-m-long nylon wire secured to the ceiling of the laboratory, and was free to adjust its yaw by driving its two propellers differentially. It was able to lock visually onto a nearby "target" (a dark edge or a bar) and to track it superaccurately [Fig. 13(c)] at angular speeds of up to 30°/s [259] (which are close to the maximum tracking speed of the human eye). Target fixation and tracking were performed regardless of the distance (up to 2.5 m) and contrast m (down to $m = 0.1$) of the target, despite the occurrence of major disturbances such as pendulum oscillations, ground effects, (gentle) taps, and light wind gusts [259].

This robot's relatively short reaction time (closed-loop time constant = 0.15 s) was due to the sensory fusion on which it was based. OSCAR was equipped with an additional rate control loop based on a microelectromechanical system (MEMS) rate gyro [Fig. 13(b)] simulating the fly's thoracic halteres, which have long been known to act like gyrometers [231]. The interplay between these two (visual and inertial) sensory modalities, combined in nested control loops [Fig. 13(b)], enhanced both the robot's stability on the yaw axis and its dynamic tracking performance [259].

OSCAR suggests that dipteran insects may in some cases be able to detect and locate targets of interest with a much greater angular accuracy than that imposed by the coarse angular sampling of their compound eyes [260]. Hovering near a tree in wait for passing mates or intruders [20], and mate fixation and pursuit [142], [143] are highly demanding detection and tracking tasks that may require both detection and location hyperacuity. Likewise, the bio-inspired inertial loop that we have added to the OSCAR feedback loop [Fig. 13(b)] to improve its stability and dynamic performances yield insights about the possible pattern of connectivity of the halteres in flies, which are known to be greatly involved in the visuo–motor control loops [261]–[263].

X. OSCAR MARK II

One of the weaknesses of the OSCAR 1 robot was that its eye was mechanically coupled to the body. A strong disturbance such as an asymmetrical gust of wind could therefore easily destabilize the body, and hence the eye, which was liable to lose sight of the target due to its small FOV. In freely flying insects, active gaze stabilization mechanisms prevent the incoming visual information from being adversely affected by disturbances such as vibrations, wind gusts, or body jerks [262]–[266]. These mechanisms play a similar role to that of the vestibulo–ocular reflex (VOR), which in many vertebrates holds gaze still in space when the head turns (e.g., [267]).

Like its forerunner, the new robot OSCAR II was still equipped with a microscanning eye endowed with hyperacuity in its small FOV (3.6°), but we introduced a one-degree-of-freedom (DOF) mechanical decoupling between the eye and the body, and implemented a VOR based on a MEMS rate gyro mounted on the body [268]. The control strategy we developed, which we called steering by gazing, consisted in maintaining the gaze automatically oriented toward the target and then ensuring that the robot's heading would catch up with the gaze, while rejecting any disturbances encountered by the body [269]. Two distinct but interdependent control schemes were implemented in this system [Fig. 14(c)]. The first one was in charge of the robot's gaze, and the other one was in charge of the robot's heading. The robot's eye dynamics were very fast in comparison with its body dynamics.

The control strategy adopted made the robot minimize its retinal error signal $\varepsilon_r = (\theta_t - \theta_g)$ [see Fig. 14(b) and (c)] and its heading error signal $(\theta_h - \theta_g)$ without requiring any information about its own absolute angular position or that of its target. The fast phase of the heading dynamics depended on the inertial sensor (the rate gyro), while the slow phase (steady state) depended on the visual

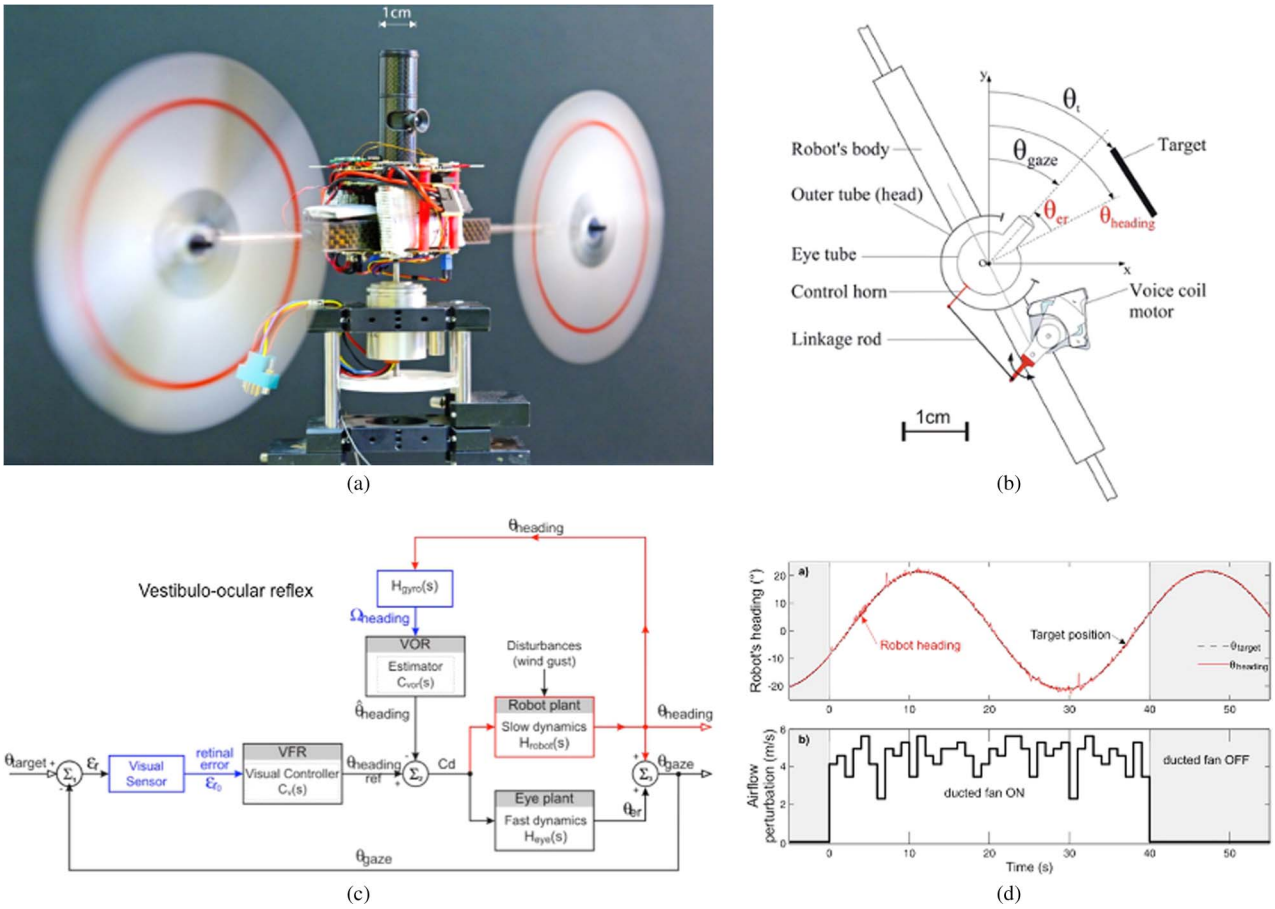

Fig. 14. ***(a) OSCAR II, like its predecessor OSCAR I, is a tethered aerial robot that orients its heading about the vertical (i.e., yaw) axis by driving its two propellers differentially, based on what it sees. The eye of OSCAR II is mechanically decoupled from the head, however. OSCAR II was mounted here on a low-friction, low-inertia resolver with which its heading could be monitored accurately. The central "eye-tube" bearing the lens and the two-pixel, piezo-translated retina (f = 10 Hz) [268] was inserted into a larger carbon tube (i.e., the "head," 10-mm diameter) mounted firmly on the robot's "body." The eye tube was thus mechanically decoupled from the body and had one degree of freedom about the yaw axis. (b) (Top view) OSCAR II with its oculomotor mechanism. The eye-in-robot angle θ_{er} (range of $\pm 35^{\circ}$) between the robot's line of sight (its gaze) and the robot's heading is controlled finely and quickly (the rise time was only 19 ms) by a micro-VCM borrowed from a hard-disk microdrive. (c) Two oculomotor reflexes, the visual fixation reflex (VFR) and the vestibulo-ocular reflex (VOR), stabilize the robot's gaze toward the target against disturbances affecting the body. The heading control system strives to realign the robot's heading with the gaze and, hence, with the visual target. (d) Actual recording of the robot's tracking performances. A gray edge was moved in the frontal plane 1 m ahead, in the presence of violent, erratic gusts of wind (up to 5 ms^{-1}) applied with a ducted fan (from 0 to 40 s) to one of the robot's propellers. (Photograph in (a) courtesy of F. Vrignaud; (b)–(d) are taken from [269].)***

sensor. OSCAR II was therefore able to reliably fixate a stationary target and reliably track a moving target despite the severe aerodynamic perturbations that were deliberately imposed on one side of its body [see Fig. 14(d)].

Unlike the other robots described above (the Robot Fly, FANIA, and OCTAVE), all of which relied on the translational OF generated by their own motion, the OSCAR robots I and II owe their excellent visual performances to the use of the purely rotational OF resulting from their retinal microscanning movements.

The development of a microgaze control system has turned out to be crucial for the visual stabilization of future robotic platforms. All-terrain wheeled robots and legged robots designed to perform terrestrial and extraterrestrial operations inherently suffer from the gaze disturbances induced by their locomotor apparatus and by the unexpected nature of the terrain they have to explore (see, e.g., [270]). Likewise, manned and unmanned air vehicles (UAVs), especially MAVs and MSVs, have to cope with the drastic disturbances caused, for instance, by fast pitch variations, wing beats, and other unpredictable aerodynamic disturbances of all kinds. Nature has taught us that these disturbances need to be compensated for at an early stage in order to reduce the load imposed on the visual system while performing its many demanding information processing tasks.

XI. CONCLUSION

Research on EMDs in both vertebrates' retina and insects' compound eye during the last six decades has involved a continuous interplay between the systems and cellular approaches. In Section V (which ends up with a summary of the biological sections of this review; see Section V-E), I reported on some findings made on flies' motion detection processes during the last 30 years using unconventional methods. The first method falls under the "systems approach," and involved recording the activity of a single identified LPTC in the housefly while stimulating two identified photoreceptor cells behind a single facet. Other methods I dealt with fall under the "cellular approach," and consisted in performing refined genetic manipulations or producing high-resolution neuroanatomical maps in the fruitfly (*Drosophila*). In some experiments, specific neurons were "genetically silenced" with a view to assessing their possible contribution to motion detection processes. Other experiments involved the use of a genetically encoded calcium indicator to record motion-related responses optically in the terminals of known cells that synapse onto the LPTCs. A third type of experiment consisted in drawing up maps of synaptic connectivity (connectomes) in order to identify the neural and synaptic components of the motion detecting circuitry.

Whereas the systems approach led to clarifying the inner processing structure of an EMD, the cellular approach led to clarifying the underlying neural hardware. The main strength of the systems approach is that it generates an elaborate model and suggests future lines of experimental study on the neural and biophysical mechanisms underlying the contributions of the various constituents of the model. But the systems approach also brings us back to what it means to "understand" a nervous system or any other information processing machine [8].

To explain how a radio set works, for example, one can opt for either a functional or structural description, where each transistor in each integrated circuit is worth describing in its own right. Likewise, an EMD subunit can be described either at the algorithmic level as an elaborate HR detector which, in each direction of motion, is split into an ON-EMD and an OFF-EMD pathway sensing the motion of bright edges and dark edges, respectively [Section V-C and Fig. 8(e)], or else one can focus on the fact that these two functional modules correspond to two distinct neuronal streams, namely L1 → T4 and L2 → T5, respectively [Section V-D and Fig. 8(e)].

Engineers with an interest in biomimetics and biorobotics will more likely be inspired by a processing structure than by the ways and means whereby it is implemented at neural level. One of the reasons for this situation is that biological organisms are weighed down with all kinds of constraints (e.g., material, metabolic, and developmental constraints) which engineers do not have to contend with, and *vice versa*. Another reason is that nature provides us with idiosyncratic neural circuitries which always result from the purposeless tinkering of evolution [271]. A given circuitry may therefore keep some vestigial elements that conflict with parsimony of design [272], [273], while misleading those who indulge in attempting to elucidate how it works.

Far from suffering from the split described above, the EMD half-detector processing structure we arrived at [Fig. 8(e)] has some major advantages at the computational, algorithmic, and implementation levels (see Section V-C). As soon as we learned about this peculiarity of the fly's EMDs to handle ON and OFF contrasts separately [225], we worked on similar lines when building our electro-optic EMDs [Fig. 9(c)] for the Robot Fly (Fig. 10), and split each EMD subunit into separate ON- and OFF-pathways.

The validity of this splitting of the fly's EMDs was confirmed recently in a series of elegant experiments involving the genetic manipulation of *Drosophila*, in which some of the neurons involved in these ON- and OFF-pathways were at last identified [Section V-D; see the colored letters in Fig. 8(e)]. All in all, these results confirm the existence of a segregation, throughout the visual pathway down to the LPTCs, of independent ON-EMDs and OFF-EMDs in the fly's motion vision processes, and settle a long-standing controversy in the field (e.g., [158] and [199] versus [207] and [274]), although some discrepancy seem to emerge again between the results of various genetic silencing experiments.

If we want to focus more closely on the biological details, the functional scheme described above [Fig. 8(e)] again serves as a worthy guide to formulating questions that still remain to be answered.

- Which neurons drive the two lateral arms [stemming from cartridge A in Fig. 8(e)] mediating the facilitatory control of the signals along the two direct arms L1–T4 and L2–T5 originating in cartridge B? We argued in Section V-D that another pair of L1 and L2 alone cannot be ascribed to this function.
- Which neurons deal with the half-wave rectifications and signal inversions required in the ON-EMDs and OFF-EMDs?
- Where exactly are the twin multipliers [Fig. 8(e)] located, which neurons drive them, and what is the exact synaptic patterns involved?
- Which neuronal chain provides inhibitory inputs to the LPTCs in the antipreferred direction?

In addition, future experiments will have to establish the extent to which the dynamics of each arm in each of the four motion subunits of an EMD (two in the preferred direction, and two in the antipreferred direction) may be affected by the animal's behavioral state [275] and its locomotion [99], [104], [276].

One particularly promising way of teasing out the processing scheme of individual EMDs more finely would consist in extending the single photoreceptor optical

microstimulation methods developed in connection with behavioral [98] or electrophysiological [124], [131], [144], [158], [204], [225] experiments and combining them with targeted genetic manipulations in *Drosophila* (e.g., [106], [108], [199], and [207]–[209]) to clarify the role of specific neurons along the motion vision pathway.

We have discovered by experience that carrying out experiments with bio-inspired sensors and robots is a more useful means of obtaining insights into basic biological problems than we ever realized before. Other authors have formulated the benefits of this approach, not to say its ultimate importance. The late Richard Feynman, for example, left a pithy note on the blackboard of his lab in 1988 saying: "What I can't create, I don't understand." And what about Carver Mead and Misha Mahowald's manifesto [277]: "It is our conviction that our ability to realize simple neural functions is strictly limited by our understanding of their organizational principles, and not by difficulties in realization. If we really understand a system, we will be able to build it. Conversely, we can be sure that a system is not fully understood until a working model has been synthesized and successfully demonstrated"?

It was again by thinking along these lines that we were recently prompted to produce a curved artificial compound eye [CurvACE; Fig. 15(a)]. Although the man-made device is still much larger (12.8 mm in width) than the fruitfly's eye, this programmable compound eye comprising 630 ommatidia and 630 photoreceptors, each of which is able to adapt independently to a vast range of ambient light, shows many of the properties of the fruitfly's eye, including its resolution and contrast transfer properties [278]. The ommatidia yield a signal acquisition bandwidth of 300 Hz, which is threefold higher than that measured in the ommatidia of fast-flying insects [279]. Any pair of neighboring equatorial ommatidia driving an EMD based on our time-of-flight scheme, with split ON- and OFF-pathways (see Section VI) is able to estimate angular velocities of a natural panorama ranging from 50 to 360°/s within a wide range of illuminance (see Fig. 6 and S9 in [278].

This compact prototype could therefore be potentially applied to the OF-based visual guidance of terrestrial and aerospace vehicles, and possibly also to collision avoidance systems for assisting visually impaired people. On the other hand, the use of handy compound eyes of this kind onboard future experimental robots will certainly help us to identify and tackle some new basic problems in animal sensory–motor control and multisensory fusion.

Our visually guided robots all make use of optic flow cues to carry out humble tasks such as detecting, locating, avoiding, and tracking environmental features, using remarkably modest resources. This approach fits a more general framework known as "active perception" [281], where the *ad hoc* movement of a motion sensor is used to constrain the sensory inputs so as to reduce the processing burden involved in perceptual tasks [282], [283].

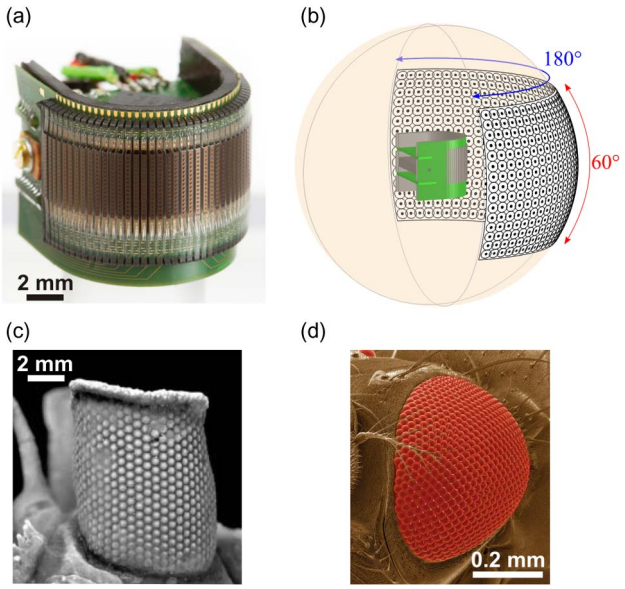

Fig. 15. *(a) Curved artificial compound eye (CurvACE) consisting of a thin 0.95-mm layer of 630 ommatidia (total weight 0.36 g) wrapped around a solid PVC substrate housing several microcontrolers and a three-axis rate gyrometer. Each ommatidium is composed of a microlens (172 μm in diameter) and a photodetector equipped with a neuromorphic analog VLSI adaptive circuit (adapted from [227]), which provides for local adaptation up to three decades of illuminance. The very short (< 1 mm) focal length of each lenslet provides for a virtually infinite depth of field, as in the fly [cf., Fig. 3(a) and (b)]. This prototype includes a communication interface such that the 42 columns of 15 photoreceptors can be read out at a high speed (up to 1500 frames/s), much faster than in another prototype which was also produced last year [280]. (b) The FOV of the eye is panoramic (180°) in the horizontal plane but limited to 60° in the vertical plane. (c) and (d) Comparison with the large compound eye of an extinct trilobite and the minute eye of the extant fruitfly Drosophila. (From [278].)*

The biomimetic principles on which robots FANIA, OCTAVE, and LORA are based (Section VIII), may pave the way for designing automatic pilots which have no need to measure the groundspeed, distance, or altitude, and can therefore do without any emissive (usually heavy, power consuming) aerospace sensors. In addition, these autopilots impose few constraints on the OF sensor's range, thanks to the feedback loops (the OF regulators) that constantly strive to produce a robot's behavior that will maintain the OF near the set point(s) [243]. Further engineering development of these systems may result in the emergence of alternatives to the conventional aerospace sensors and autopilots, and various applications in the fields of air and space technology have been envisaged (e.g., [284]–[287]), as occurred in the case of the horizon sensor inspired by the dragonfly ocelli [288].

The fly-inspired retinal microscanner on which the SCANIA, OSCAR I, and OSCAR II robots are based (Sections IX and X) may pave the way for low-cost, highly

accurate nonemissive detection and tracking systems, as needed, for example, in aircraft collision avoidance systems [289] or power line detection systems onboard full-scale helicopters [258]. One biological benefit of these technological developments is that they generate hypotheses about the whys and wherefores of the fly retinal microscanner (Fig. 4). Future behavioral tests will tell us whether flies use this intriguing contraption to better detect, locate, and track quarries or mates. But even if this hypothesis turns out to be wrong, it will have led to stimulating hints for new robotic system design.

The latest development on these lines was the Vibrating Optical Device for the Kontrol of Autonomous (VODKA) sensor, which is able to locate a contrasting edge with a resolution up to 900-fold greater than its static resolution, regardless of the scanning law imposed on the retina [290] (see also [198]). Hyperacuity is obtained at a low cost, thus opening new vistas for the fine visuo–motor control of robotic platforms, with potential applications in the fields of metrology, astronomy, robotics, and automotive and aerospace engineering.

These are some of the many lessons which can be learned from the "humble representatives of life." Building a smart sensory front end can help to relieve the subsequent computational burden. "Put your money in smart sensors and not in the computer behind" could be the motto. Flying insects are not only the oldest fly-by-wire aircraft, but also they are able to achieve a great deal with very few resources: few pixels in the eyes, and few neurons in the brain. They can no doubt keep telling us some special secrets in the realm of sensory–motor control [75], [76], [81], as they have done in the field of advanced materials [74], [291]. The millions of insect species which exist in the world constitute a gigantic untapped reservoir of ideas for sophisticated microsensors, microactuators, and smart guidance principles. The biorobotic approach provides neurobiologists and neuroethologists with clues for identifying and investigating worthwhile problems, while at the same time suggesting ways of designing sensors and autopilots that benefit from the millions of centuries of experience acquired in the course of biological evolution. Perhaps the greatest advantage of this approach is that it breaks down barriers and creates a veritable synergy between scientific disciplines that still talk too little to one another, such as: ethology, neurobiology, ecology, genetics, optics, mechanics, electronics, informatics, control engineering, aerospace, etc. This truly transdisciplinary approach is therefore likely to boost the progress of several branches of scientific research, as well as holds great promise for developing the smart vehicles and microvehicles of the future. ■

Acknowledgment

This paper is dedicated to the memory of Prof. Dezsö Varju (1932–2013) who was a Professor of Biological Cybernetics at the University of Tübingen, Tübingen, Germany, from 1968 to 1997 [292].

The author would like to thank many colleagues from several laboratories with whom he has worked over the years: K. G. Götz, K. Kirschfeld, R. Hardie, B. Minke, W. Ribi, P. McIntyre, K. Hausen, A. Münster, M. Feiler, D. Stavenga, A. Riehle, M. Wilcox, A. Le Nestour, S. Picaud, H. J. Wunderer, A. Mücke, A. Totin, R. Chagneux, J. M. Pichon, C. Blanes, N. Martin, F. Mura, H. Sturm, A. Weber, T. Netter, R. Navarro, Y. Hanyu, S. Viollet, F. Ruffier, T. Mukai, F. Aubépart, M. El Farji, J. Michelis, M. Pudas, S. Amic, D. Dray, J. Serres, G. Masson, L. Kerhuel, G. Portelli, F. Roubieu, R. Juston, F. Expert, D. Floreano, G. Sabiron, F. Colonnier, M. Menouni, M. Boyron, F. Paganucci, and J. Diperi. He would also like to thank M. Boyron for his help with the figures and J. Blanc for improving the English in this manuscript. The author is most grateful to all three anonymous reviewers for their constructive comments.

REFERENCES

[1] J. Y. Lettvin, H. R. Maturana, W. S. McCulloch, and W. H. Pitts, "What the frog's eye tells the frog's brain," *Proc. IRE*, vol. 47, no. 11, pp. 1940–1951, Nov. 1959.

[2] W. H. Warren, B. A. Kay, D. Zosh, P. Duchon, and S. Sahuc, "Optic flow is used to control human walking," *Nature Neurosci.*, vol. 4, pp. 213–216, 2001.

[3] W. K. Page and C. J. Duffy, "Cortical neural responses to optic flow are shaped by visual strategies for steering," *Cereb. Cortex*, vol. 18, no. 4, pp. 727–739, 2008.

[4] A. Borst and T. Euler, "Seeing things in motion: Models, circuits, mechanisms," *Neuron*, vol. 71, pp. 974–994, 2011.

[5] C. Gilbert, "Brain connectivity: Revealing the fly visual motion circuit," *Current Biol.*, vol. 23, no. 18, pp. R851–R853, Aug. 2013.

[6] R. Masland, "Accurate maps of visual circuitry," *Nature*, vol. 500, no. 7461, Aug. 2013.

[7] W. Reichardt, "Autocorrelation, a principle for the evaluation of sensory information by the central nervous system," in *Sensory Communication*, M. A. Rosenblith, Ed. Cambridge, MA, USA: MIT Press, 1961, pp. 303–317.

[8] D. C. Marr and T. Poggio, "From understanding computation to understanding neural circuitry," *Neurosci. Res. Progr. Bull.*, vol. 15, pp. 470–488, 1977.

[9] A. V. Herz, T. Gollisch, C. Machens, and D. Jaeger, "Modeling single-neuron dynamics and computations: A balance of detail and abstraction," *Science*, vol. 314, pp. 80–85, 2006.

[10] B. Hassenstein and W. Reichardt, "Systemtheoretische Analyse der Zeit-, Reihenfolgen und Vorzeichenauswertung bei der Bewegungsperzeption des Rüsselkäfers Chlorophanus," *Z. Naturforschung B*, vol. 11, pp. 513–552, 1956.

[11] K. G. Götz, "Optomotorische Untersuchung des visuellen Systems einiger Augenmutanten der Fruchtfliege Drosophila," *Biol. Cybern.*, vol. 2, pp. 77–92, 1964.

[12] W. Reichardt, "Movement perception in insects," in *Processing of Optical Data by Organisms and by Machines*, R. W. Ed., Ed. New York, NY, USA: Academic, 1969, pp. 465–493.

[13] T. Poggio and W. Reichard, "Visual control of orientation behavior in the fly. II. Towards the underlying neural interactions," *Quart. Rev. Biophys.*, vol. 9, pp. 377–438, 1976.

[14] E. Buchner, "Behavioural analysis of spatial vision in insects," in *Photoreception and Vision in Invertebrates*, M. Ali, Ed. New York, NY, USA: Plenum, 1984, pp. 561–621.

[15] D. N. Lee, "Visual information during locomotion," in *Perception: Essays in Honour of James Gibson*, R. B. Macleod and H. L. Pick, Eds. Ithaca, NY, USA: Cornell Univ. Press, 1974, pp. 250–267.

[16] C. J. Duffy, "Optic flow analysis for self-movement perception," *Intern. Rev. Neurobiol*, vol. 44, pp. 199–218, 2000.

[17] J. S. Kennedy, "Visual responses of flying mosquitoes," *Proc. Zool. Soc. Lond.*, vol. 109, pp. 221–242, 1939.

[18] J. S. Kennedy, "The migration of the desert locust," *Phil. Trans. Roy. Soc. Lond. B*, vol. 235, pp. 163–290, 1951.

[19] G. Portelli, F. Ruffier, F. L. Roubieu, and N. Franceschini, "Honeybees' speed depends on dorsal as well as lateral, ventral and frontal optic flows," *Plos One*, vol. 6, no. 5, pp. 1–10, 2011.

[20] T. S. Collett and M. F. Land, "Visual control of flight behaviour in the hoverfly Syritta pipiens L.," *J. Comparative Physiol. A*, vol. 99, no. 1, pp. 1–66, 1975.

[21] H. Wagner, "Flight performance and visual control of flight of the free-flying housefly (Musca Domestica L.)," *Phil. Trans. Roy. Soc. London. B*, vol. 312, no. 1158, pp. 527–595, 1986.

[22] J. H. V. Hateren van and C. Schilstra, "Blowfly flight and optic flow II. Head movements during flight," *J. Exp. Biol.*, vol. 202, pp. 1491–1500, 1999.

[23] T. Netter and N. Franceschini, "A robotic aircraft that follows terrain using a neuromorphic eye," in *Proc. IEEE/RSJ Int. Conf. Intell. Robots Syst.*, Lausanne, Switzerland, 2002, vol. 1, pp. 129–134.

[24] W. F. Green, Y. Oh, and G. Barrows, "Flying insect inspired vision for autonomous axial robot maneuvers in near earth environments," in *Proc. IEEE Int. Conf. Robot. Autom.*, 2004, pp. 2343–2352.

[25] J.-C. Zufferey, A. Klaptocz, A. Beyeler, J.-D. Nicoud, and D. Floreano, "A 10-gram vision-based flying robot," *Adv. Robot.*, vol. 2, no. 14, pp. 1671–1684, 2007.

[26] S. Bermudezi Badia, P. Pyk, and P. F. Verschure, "A fly-locust based neuronal control system applied to an unmanned aerial vehicle: The invertebrate neuronal principles for course stabilization, altitude control and collision avoidance," *Int. J. Robot. Res.*, vol. 26, pp. 759–772, 2007.

[27] J. Conroy, G. Grémillon, B. Ranganathan, and J. S. Humbert, "Implementation of wide-field integration of optic flow for autonomous quadrotor navigation," *Autonom. Robots*, vol. 27, pp. 189–198, 2009.

[28] D. Lentink, S. R. Jongerius, and N. L. Bradshaw, "The scalable design of flapping micro-air vehicles inspired by insect flight," in *Flying Insects and Robots*, D. Floreano, J.-C. Zufferey, M. V. Srinivasan, and C. Ellington, Eds. Berlin, Germany: Springer-Verlag, 2009, pp. 185–205.

[29] G. C. H. De Croon, K. M. E. De Clercq, R. Ruijsink, and B. Remes, "Design, aerodynamics, vision-based control of the del-fly," *Int. J. Micro Air Veh.*, vol. 1, pp. 71–98, 2009.

[30] H. Liu, "Micro air vehicles (MAV section)," in *Encyclopedia of Aerospace Engineering*. New York, NY, USA: Wiley, 2010.

[31] M. Keennon, K. Klingebiel, and H. Won, "Development of the nano hummingbird: A tailless flapping wing micro air vehicle," in *Proc. 50th AIAA Aerosp. Sci. Meeting*, Jan. 2012, pp. 1–24.

[32] R. Wood, B. Finio, M. Karpelson, K. Ma, N. O. Pérez-Arancibia, P. S. Streetharan, H. Tanaka, and J. P. Whitney, "Progress on 'pico' air-vehicles," *Int. J. Robot. Res.*, vol. 31, no. 11, pp. 1292–1302, Sep. 2012.

[33] D. Mackenzie, "A flapping of wings," *Science*, vol. 335, pp. 1430–1433, 2012.

[34] K. Y. Ma, P. Chirarattananon, S. B. Fuller, and R. J. Wood, "Controlled flight of a biologically inspired, insect-scale robot," *Science*, vol. 340, pp. 603–607, 2013.

[35] B. Webb, "Robots in invertebrate neuroscience," *Nature*, vol. 147, pp. 359–363, 2002.

[36] N. Franceschini, J. M. Pichon, and C. Blanes, "From insect vision to robot vision," *Philos. Trans. Roy. Soc. Lond. B*, vol. 337, no. 1281, pp. 283–294, 1992.

[37] D. Coombs and K. Roberts, "'Bee-bot': Using peripheral optical flow to avoid obstacles," in *Proc. Intell. Robot. Comput. Vis.*, 1992, vol. 1835, pp. 714–725.

[38] G. Sandini, J. Santos-Victor, F. Curotto, and S. Garibaldi, "Robotic bees," in *Proc. IEEE/RSJ Int. Conf. Intell. Robots Syst.*, New York, NY, USA, 1993, vol. 1, pp. 629–635.

[39] R. D. Beer, R. E. Ritzmann, and T. McKenna, *Biological Neural Networks in Invertebrate Neuroethology and Robotics*. New York, NY, USA: Academic, 1993.

[40] B. Webb, "Robotic experiments in cricket phonotaxis," in *From Animals to Animats III*, D. Cliff, P. Husbands, J. A. Meyer, and S. W. Wilson, Eds. Cambridge, MA, USA: MIT Press, 1994, pp. 45–54.

[41] F. Mondada, E. Franzi, and P. Ienne, "Mobile robot miniaturization: A tool for investigation in control algorithms," in *Experimental Robotics III*. London, U.K.: Springer-Verlag, 1994, pp. 501–513.

[42] M. S. Triantafyllou and G. S. Triantafyllou, "An efficient swimming machine," *Sci. Amer.*, vol. 272, no. 3, pp. 64–70, 1995.

[43] F. Pfeiffer, F. J. Eltze, and H. J. Weidemann, "Six-legged technical walking machine considering biological principles," *Robot. Autonom. Syst.*, vol. 14, pp. 223–232, 1995.

[44] F. Mura and N. Franceschini, "Obstacle avoidance in a terrestrial mobile robot provided with a scanning retina *Proc. IEEE Int. Symp. Intell. Veh.*, 1996, pp. 47–52.

[45] K. S. Espenshied, R. D. Quinn, H. J. Chiel, and R. D. Beer, "Biologically-based distributed control and local reflexes improve rough terrain locomotion in a hexapod robot," *Robot. Autonom. Syst.*, vol. 18, pp. 59–64, 1996.

[46] S. Viollet and N. Franceschini, "Visual servo system based on a biologically-inspired scanning sensor," in *Sensor Fusion and Decentralized Control*, vol. 3839, G. McKee and P. Schenker, Eds. Bellingham, WA, USA: SPIE, 1999, pp. 144–155.

[47] D. Lambrinos, R. Möller, T. Labhart, R. Pfeifer, and R. Wehner, "A mobile robot employing insect strategies for navigation," *Robot. Autonom. Syst.*, vol. 30, pp. 39–64, 2000.

[48] N. Kato, "Control performance in horizontal plane of a fish robot with mechanical pectoral fins," *IEEE J. Ocean. Eng.*, vol. 25, no. 1, pp. 121–129, Jan. 2000.

[49] F. Iida and D. Lambrinos, "Navigation in an autonomous flying robot by using a biologically inspired visual odometer," in *Sensor Fusion and Decentralized Control in Robotic Systems III*, vol. 4196, G. T. McKee and P. S. Schenker, Eds. Bellingham, WA, USA: SPIE, 2000, p. 86.

[50] R. R. Harrison and C. Koch, "A silicon implementation of the fly's optomotor control system," *Neural Comput.*, vol. 12, pp. 2291–2304, 2000.

[51] F. Ruffier and N. Franceschini, "OCTAVE: A bioinspired visuo-motor control system for the guidance of micro-air vehicles," in *Bioengineered and Bioinspired Systems*, vol. 5119, A. Rodriguez-Vasquez, D. Abbott, and R. Carmona, Eds. Bellingham, WA, USA: SPIE, 2003, pp. 1–12.

[52] C. Rind, "Bioinspired sensors: From insect eyes to robot vision," in *Methods in Insect Sensory Neuroscience*, T. A. Christensen, Ed. Boca Raton, FL, USA: CRC Press, 2004, pp. 213–234.

[53] M. Schilling, T. Hoinville, J. Schmitz, and H. Cruse, "Walknet, a bio-inspired controller for hexapod walking," *Biol. Cybern.*, vol. 107, no. 4, pp. 397–419, 2013.

[54] H. Hu, "Biologically inspired design of autonomous robotic fish at Essex," in *Proc. IEEE SMC UK-RI Conf.*, Sheffield, U.K., 2006, pp. 1–8.

[55] S. Bouabdallah and R. Siegwart, "Design and control of an indoor coaxial helicopter," in *Proc. IEEE/RSJ Int. Conf. Robot. Syst.*, Beijing, 2006, pp. 2930–2935.

[56] A. J. Ijspeert, A. Crespi, D. Ryczko, and J. M. Cabelguen, "From swimming to walking with a salamander robot driven by a spinal cord model," *Science*, vol. 315, no. 5817, pp. 1416–1420, 2007.

[57] S. Kim, M. Spenko, S. Trujillo, B. Heyneman, D. Santos, and M. R. Cutkosky, "Smooth vertical surface climbing with directional adhesion," *IEEE Trans. Robot.*, vol. 24, no. 1, pp. 65–74, Feb. 2008.

[58] F. Kendoul, I. Fantoni, and K. Nonami, "Optic flow-based vision system for autonomous 3D localization and control of small aerial vehicles," *Robot. Autonom. Syst.*, vol. 57, pp. 591–602, 2009.

[59] C. Laschi, M. Cianchetti, B. Mazzolai, L. Margheri, M. Follador, and P. Dario, "Soft robot arm inspired by the octopus," *Adv. Robot.*, vol. 26, no. 7, pp. 709–727, 2012.

[60] F. L. Roubieu, J. Serres, N. Franceschini, F. Ruffier, and S. Viollet, "A fully autonomous hovercraft inspired by bees: Wall-following and speed control in straight and tapered corridors," in *Proc. IEEE Int. Conf. Robot. Biomimetics*, Guangzhou, China, 2012, pp. 1311–1318.

[61] V. Braitenberg, *Vehicles*. Cambridge, MA, USA: MIT Press, 1984.

[62] M. Raibert, *Legged Robots That Balance*. Cambridge, MA, USA: MIT Press, 1986.

[63] P. Maes, *Designing Autonomous Agents: Theory and Practice From Biology to Engineering and Back*. Cambridge, MA, USA: MIT Press, 1990.

[64] R. A. Brooks, "New approaches to robotics," *Science*, vol. 253, pp. 1227–1232, 1991.

[65] S. Hirose, *Biologically Inspired Robots*. Oxford, U.K.: Oxford Univ. Press, 1993.

[66] R. D. Beer, H. J. Chiel, R. D. Quinn, and R. E. Ritzmann, "Biorobotic approaches to the study of motor systems," *Current Opinion Neurobiol.*, vol. 8, pp. 777–782, 1998.

[67] N. Franceschini, "Engineering applications of small brains," *Future Electron Devices J.*, vol. 7, pp. 38–52, 1996.

[68] M. V. Srinivasan and S. Venkatesh, *From Living Eyes to Seeing Machines*. Oxford, U.K.: Oxford Univ. Press, 1997.

[69] R. Arkin, *Behavior-Based Robotics*. Cambridge, MA, USA: MIT Press, 1998.

[70] R. A. Brooks, *Cambrian Intelligence*. Cambridge, MA, USA: MIT Press, 1999.

[71] M. A. Lewis and M. A. Arbib, "Introduction to the special issue on biomorphic robots,"

Autonom. Robots, vol. 7, no. 3, pp. 207–209, 1999.

[72] C. Chang and P. Gaudiano, "Biomimetic robotics," *Robot. Autonom. Syst.*, vol. 30, no. 1, pp. 1–2, 2000.

[73] B. Webb and T. Consi, *Biorobotics*. Cambridge, MA, USA: MIT Press, 2001.

[74] W. Nachtigall, *Bionik*, 2nd ed. Berlin, Germany: Springer-Verlag, 2002.

[75] J. Ayers, J. Davis, and A. Rudolph, *Neurotechnology for Biomimetic Robots*. Cambridge, MA, USA: MIT Press, 2002.

[76] F. G. Barth, J. A. C. Humphrey, and T. W. Secomb, *Sensors and Sensing in Biology and Engineering*. Berlin, Germany: Springer-Verlag, 2003.

[77] A. Guillot and J. A. Meyer, "Biomimetic robotics," *Robot. Autonom. Syst.*, vol. 50, no. 4, pp. 129–230, 2005.

[78] D. Floreano and C. Mattiussi, *Bio-Inspired Artificial Intelligence: Theories, Methods and Technologies*. Cambridge, MA, USA: MIT Press, 2008.

[79] D. Floreano, D. J. C. Zufferey, M. V. Srinivasan, and C. Ellington, *Flying Insects and Robots*. Berlin, Germany: Springer-Verlag, 2009.

[80] A. Guillot and J. A. Meyer, *How to Catch a Robot Rat. When Biology Inspires Innovation*. Cambridge, MA, USA: MIT Press, 2010.

[81] F. Barth, P. Humphrey, and M. V. Srinivasan, *Frontier in Sensing: From Biology to Engineering*. Berlin, Germany: Springer-Verlag, 2012.

[82] R. F. Boyer, C. Stefanini, F. Ruffier, and S. Viollet, "Special issue featuring selected papers from the International Workshop on Bio-Inspired Robots (Nantes, France, 6–8 April 2011)," *Bioninsp. and Biomin*, vol. 5, p. 7, 2012, 020201.

[83] R. J. Martin-Palma and A. Lakhtakia, "Special issue on biomimetic sensors," *IEEE Sensors J.*, vol. 12, no. 2, p. 271, Feb. 2012.

[84] A. J. Ijspeert, S. Grillner, and P. Dario, "Foreword for the special issue on Lamprey and Salamander robots and the central nervous system," *Biol. Cybern.*, vol. 107, pp. 495–496, 2013.

[85] D. De Rossi and M. Pieroni, "Grand challenge in biomimetics," *Front. Bioeng. Biotechnol.*, Jun. 2013, DOI: 10.3389/fbioe.2013.00003.

[86] N. F. Lepora, P. Verschure, and T. J. Prescott, "The state of the art in biomimetics," *Bioinspiration Biomimetics*, vol. 8, 2013, DOI: 10.1088/1748-3182/8/1/013001.

[87] G. Indiveri and R. Douglas, "Neuromorphic vision sensors," *Science*, vol. 288, pp. 1189–1190, 2000.

[88] C. A. Mead, *Analog VLSI and Neural Systems*. Reading, MA, USA: Addisson-Wesley, 1989.

[89] J. Schemmel, J. Fieres, and K. Meier, "Wafer-scale integration of analog neural networks," in *Proc. IEEE Int. Joint Conf. Neural Netw.*, 2008, pp. 431–438.

[90] R. Etienne-Cummings, "Intelligent robot vision sensors in VLSI," *Autonom. Robots*, vol. 7, pp. 225–237, 1999.

[91] C. Mead, "Neuromorphic electronic systems," *Proc IEEE*, vol. 78, no. 10, pp. 1629–1636, Oct. 1990.

[92] R. Douglas, M. Mahowald, and M. C. Mead, "Neuromorphic engineering," *Annu. Rev. Neurosci.*, vol. 18, pp. 255–281, 1995.

[93] W. Reichardt, "Movement perception in insects," in *Processing Optical Data by Organisms and Machines*, W. Reichardt, Ed. New York, NY, USA: Academic, 1969, pp. 465–493.

[94] K. G. Götz, "Die optischen Übertragungseigenschaften der Komplexaugen von Drosophila," *Biol. Cybern.*, vol. 2, pp. 215–221, 1965.

[95] E. Buchner, "Elementary movement detectors in an insect visual system," *Biol. Cybern.*, vol. 24, pp. 85–101, 1976.

[96] M. Heisenberg and R. Wolf, *Vision in Drosophila*. New York, NY, USA: Springer-Verlag, 1984.

[97] B. Hassenstein, "Ommatidienraster und afferente Bewegungs-integration," *J. Comparative Physiol. A*, vol. 33, pp. 301–326, 1951.

[98] K. Kirschfeld, "The visual system of Musca: Studies on optics, structure and function," in *Information Processing in the Visual Systems of Arthropods*, R. Wehner, Ed. Berlin, Germany: Springer-Verlag, 1972, pp. 61–74.

[99] M. E. Chiappe, J. D. Seelig, M. B. Reiser, and V. Jayaraman, "Walking modulates speed sensitivity in Drosophila motion vision," *Current Biol.*, vol. 20, pp. 1470–1475, 2010.

[100] M. Heisenberg, R. Wonnenberger, and R. Wolf, "Optomotor blind (H31)—A Drosophila mutant of the lobula plate giant neurons," *J. Comparative Physiol.*, vol. 124, pp. 287–296, 1978.

[101] G. Geiger and D. R. Nässel, "Visual orientation behavior of flies after selective laser beam ablation of interneurones," *Nature*, vol. 293, pp. 398–399, 1981.

[102] K. Hausen and C. Wehrhahn, "Microsurgical lesion of horizontal cells changes optomotor yaw responses in the blowfly Calliphora erythrocephala," *Proc. Roy. Soc. Lond. B*, vol. 219, pp. 211–216, 1983.

[103] K. Hausen and C. Wehrhahn, "Neural circuits mediating visual flight control in flies: I. Quantitative comparison of neural and behavioural response characteristics," *J. Neurosci.*, vol. 9, pp. 3828–3836, 1989.

[104] G. Maimon, A. D. Straw, and M. H. Dickinson, "Active flight increases the gain of visual motion processing in Drosophila," *Nature Neurosci.*, vol. 13, no. 3, pp. 393–401, 2010.

[105] M. Wernet and C. Desplan, "Building a retinal mosaic: Cell-fate decision in the fly eye," *Trends Cell Biol.*, vol. 14, no. 10, pp. 576–584, 2004.

[106] H. Eichner, M. Joesch, B. Schnell, D. F. Reiff, and A. Borst, "Internal structure of the fly elementary motion detector," *Neuron*, vol. 70, pp. 1155–1164, 2011.

[107] M. Joesch, F. Weber, H. Eichner, and A. Borst, "Functional specialization of parallel motion detection circuits in the fly," *J. Neurosci.*, vol. 33, pp. 902–905, 2013.

[108] M. S. Maisak, J. Haag, G. Ammer, E. Serbe, M. Meier, A. Leonhardt, T. Schilling, A. Bahl, G. M. Rubin, A. Nern, B. J. Dickson, D. F. Reiff, E. Hopp, and A. Borst, "A directional tuning map of Drosophila elementary motion detectors," *Nature*, vol. 500, pp. 212–216, Aug. 2013.

[109] R. C. Hardie, "Phototransduction mechanisms in Drosophila microvillar photoreceptors," *Membrane Transp. Signal.*, 2011, DOI: 10.1002/wmts.20.

[110] N. C. Strausfeld, *Atlas of an Insect Brain*. Berlin, Germany: Springer-Verlag, 1976.

[111] N. Strausfeld, "Beneath the compound eye: Neuroanatomical analysis and physiological correlates in the study of insect vision," in *Facets of Vision*, D. G. Stavenga and R. C. Hardie, Eds. Berlin, Germany: Springer-Verlag, 1989, pp. 317–359.

[112] K. F. Fishbach and A. P. M. Dittrich, "The optic lobe of Drosophila melanogaster, I: A Golgi analysis of wild-type structure," *Cell Tissue Res.*, vol. 258, pp. 441–475, 1989.

[113] N. Franceschini and K. Kirschfeld, "Etude optique *in vivo* des éléments photorécepteurs dans l'oeil composé de Drosophila," *Biol. Cybern.*, vol. 8, no. 1, pp. 1–13, 1971.

[114] N. Franceschini, K. Kirschfeld, and B. Minke, "Fluorescence of photoreceptor cells observed *in vivo*," *Science*, vol. 213, no. 4513, pp. 1264–1267, 1981.

[115] R. Hardie, N. Franceschini, and P. McIntyre, "Electrophysiological analysis of fly retina II: Spectral and polarisation sensitivity in R7 and R8," *J. Comparative Physiol. A*, vol. 133, no. 1, pp. 23–39, 1979.

[116] N. Franceschini, R. Hardie, W. Ribi, and K. Kirschfeld, "Sexual dimorphism in a photoreceptor," *Nature*, vol. 291, no. 5812, pp. 241–244, 1981.

[117] R. C. Hardie, "Electrophysiological analyses of the fly retina I. Comparative properties of R1–6 and R7 and 8," *J. Comparative Physiol. A*, vol. 129, pp. 19–33, 1979.

[118] R. Hardie, "Functional organization of the fly retina," in *Progress in Sensory Physiology*, vol. 5, D. Ottosson, Ed. Berlin, Germany: Springer-Verlag, 1985, pp. 2–79.

[119] M. Järvilehto and F. Zettler, "Localized intracellular potentials and pre- and postsynaptic components in the external plexiform layer of an insect retina," *Z. Vergl. Physiol.*, vol. 75, pp. 422–440, 1971.

[120] S. Laughlin, "The role of parallel channels in early visual processing by the arthropod compound eye," in *Photoreception and Vision in Invertebrates*, M. A. Ali, Ed. New York, NY, USA: Plenum, 1984, pp. 457–481.

[121] J. Howard, B. Blakeslee, and S. B. Laughlin, "The intracellular pupil mechanism and photoreceptor signal: Noise ratios in the fly Lucilia cuprina," in *Proc. Roy. Soc. Lond. B*, vol. 231, pp. 415–435, 1987.

[122] S. Picaud, H. J. Wunderer, and N. Franceschini, "Dye-induced photopermeabilisation and photodegeneration of neurons: A lesion technique useful for neuronal tracing," *J. Neurosci. Methods*, vol. 33, pp. 101–112, 1990.

[123] M. Wilcox and N. Franceschini, "Illumination induces dye incorporation in photoreceptor cells," *Science*, vol. 225, pp. 851–854, 1984.

[124] N. Franceschini, "Early processing of colour and motion in a mosaic visual system," *Neurosci. Res.*, vol. 2, no. Suppl., pp. S17–S49, 1985.

[125] N. Franceschini, "Sampling of the visual environment by the compound eye of the fly: Fundamentals and applications," in *Photoreceptor Optics*, A. Snyder and R. Menzel, Eds. Berlin, Germany: Springer-Verlag, 1975, pp. 360–390.

[126] M. Heisenberg and E. Buchner, "The role of retinal cell types in visual behavior of Drosophila melanogaster," *J. Comparative Physiol. A*, vol. 117, pp. 127–162, 1977.

[127] S. Yamaguchi, R. Wolf, C. Desplan, and M. Heisenberg, "Motion vision is independent of color vision in Drosophila," *Proc. Nat. Acad. Sci. USA*, vol. 105, pp. 4910–4915, 2008.

[128] N. Franceschini, "Chromatic organization and sexual dimorphism of the fly retinal mosaic," in *Photoreceptors*, A. Borsellino and L. Cervetto, Eds. New York, NY, USA: Plenum, 1984, pp. 319–350.

[129] S. Takemura, T. Karuppudurai, C. Y. Ting, E. Z. Lu, C. H. Lee, and I. A. Meinertzhagen, "Cholinergic circuits integrate neighboring visual signals in a Drosophila Motion detection pathway," *Current Biol.*, vol. 21, pp. 2077–2084, Dec. 2011.

[130] S. Takemura, A. Bharioke, Z. Lu, A. Nern, S. Vitaladevuni, P. K. Rivlin, W. T. Katz, D. J. Olbris, S. M. Plaza, P. Winston, T. Zhao, J. A. Horne, R. D. Fetter, S. Takemura, K. Blazek, L.-A. Chang, O. Ogundeyi, M. A. Saunders, V. Shapiro, C. Sigmund, G. M. Rubin, L. K. Scheffer, I. A. Meinertzhagen, and D. B. Chklovskii, "A visual motion detection circuit suggested by Drosophila connectomics," *Nature*, vol. 500, no. 7461, pp. 175–181, Aug. 2013.

[131] A. Riehle and N. Franceschini, "Motion detection in flies: Parametric control over ON-OFF pathways," *Exp. Brain Res.*, vol. 54, no. 2, pp. 390–394, 1984.

[132] K. Kirschfeld and N. Franceschini, "Optische Eigenschaften der Ommatidien im Komplexauge von Musca," *Biol. Cybern.*, vol. 5, pp. 47–52, 1968.

[133] K. Kirschfeld, N. Franceschini, and B. Minke, "Evidence for a sensitizing pigment in fly photoreceptors," *Nature*, vol. 269, no. 5627, pp. 386–390, 1977.

[134] P. Vigier, "Mécanisme de la synthèse des impressions lumineuses recueillies par les yeux composés des Diptères," *C. R. Acad. Sci.*, vol. 148, pp. 1221–1223, 1909.

[135] V. Braitenberg, "Patterns of projection in the visual system of the fly: Retina-lamina projections," *Exp. Brain Res.*, vol. 3, pp. 271–298, 1967.

[136] K. Kirschfeld, "Die Projektion der optischen Umwelt auf das Raster der Rhabdomere im Komplexauge von Musca," *Exp. Brain Res.*, vol. 3, pp. 248–270, 1967.

[137] J. H. V. Hateren van, "Electrical coupling of neuro-ommatidial photoreceptor cells in the blowfly," *J. Comparative Physiol. A*, vol. 158, pp. 795–811, 1986.

[138] J. H. V. Hateren van, "Neural superposition and oscillations in the eye of the blowfly," *J. Comparative Physiol. A*, vol. 161, pp. 849–855, 1987.

[139] M. Juusola, R. O. Uusitalo, and M. Weckström, "Transfer of graded potentials at the photoreceptor-interneuron synapse," *J. Gen. Physiol.*, vol. 105, pp. 117–148, 1995.

[140] R. C. Hardie, N. Franceschini, W. Ribi, and K. Kirschfeld, "Distribution and properties of sex-specific photoreceptors in the fly Musca domestica," *J. Comparative Physiol.*, vol. 145, pp. 139–152, 1981.

[141] K. Hausen and N. J. Strausfeld, "Sexually dimorphic interneuron arrangement in the fly visual system," *Proc. Roy. Soc. Lond. B*, vol. 208, pp. 57–71, 1980.

[142] C. Wehrhahn, "Sex-specific differences in the chasing behaviour of houseflies (Musca)," *Biol. Cybern.*, vol. 32, no. 4, pp. 239–241, 1979.

[143] N. Boeddeker, R. Kern, and M. Egelhaaf, "Chasing a dummy target: Smooth pursuit and velocity control in male blowflies," *Proc. Roy. Soc. Lond. B*, vol. 270, pp. 393–399, 2003.

[144] K. N. Franceschini, "Sequence-discriminating neural network in the eye of the fly," in *Analysis and Modeling of Neural Systems*, F. H. K. Eeckman, Ed. Norwell, MA, USA: Kluwer, 1992, pp. 142–150.

[145] K. Kirschfeld and N. Franceschini, "Ein Mechanismus zur Steuerung des Lichtflusses in den Rhabdomeren des Komplexauges von Musca," *Biol. Cybern.*, vol. 6, pp. 13–22, 1969.

[146] N. Franceschini, "Pupil and pseudopupil in the compound eye of Drosophila," in *Information Processing in the Visual Systems of Arthropods*, R. Wehner, Ed. Berlin, Germany: Springer-Verlag, 1972, pp. 75–82.

[147] N. Franceschini and K. Kirschfeld, "Le contrôle automatique du flux lumineux dans l'oeil composé des diptères: Propriétés spectrales, statiques et dynamiques du mécanisme," *Biol. Cybern.*, vol. 21, pp. 181–203, 1976.

[148] J. G. H. Roebroek and D. G. Stavenga, "On the effective optical density of the pupil mechanism in fly photoreceptors," *Vis. Res.*, vol. 30, no. 8, pp. 1235–1242, 1990.

[149] N. Franceschini, "Die Regelung des Lichtflusses im Komplexauge der Dipteren: Ein 'Automatic gain control'," presented at the Jahrestagung der Deutschen Gesellschaft für Biophysik e.V., Abstract, p. 12, Freiburg, Germany, Oct. 1974.

[150] K. Kirschfeld and K. Vogt, "Calcium ions and pigment migration in fly photoreceptors," *Naturwissenschaften*, vol. 67, no. 10, pp. 516–517, 1980.

[151] A. Satoh, X. Bingbing, H. Xia, and D. F. Ready, "Calcium-activated myosin V closes the Drosophila pupil," *Current Biol.*, vol. 18, pp. 951–955, 2008.

[152] J. Burtt and J. Patterson, "Internal muscle in the eye of an insect," *Nature*, vol. 228, pp. 183–184, 1970.

[153] R. Hengstenberg, "Das Augenmuskelsystem der Stubenfliege Musca domestica," *Biol. Cybern.*, vol. 9, no. 2, pp. 56–77, 1971.

[154] N. Franceschini, "Combined optical, neuroanatomical, electrophysiological and behavioural studies on signal processing in the fly compound eye," in *Biocybernetics of Vision: Integrative Mechanisms and Cognitive Processes*, C. Taddei-Ferretti, Ed. London, U.K.: World Scientific, 1998, pp. 341–361.

[155] N. Franceschini and R. Chagneux, "Repetitive scanning in the fly compound eye," G. Thieme, Stuttgart, Germany, Göttingen Neurobiol. Rep., 1997, p. 279.

[156] W. O. Landolt and A. Mitros, "Visual sensor with resolution enhancement by mechanical vibrations," *Autonom. Robots*, vol. 11, pp. 233–239, 2001.

[157] M. Egelhaaf and A. Borst, "Movement detection in arthropods," in *Visual Motion and Its Role in the Stabilization of Gaze*, F. A. Miles and G. Wallman, Eds. Amsterdam, The Netherlands: Elsevier, 1993, pp. 53–77.

[158] N. Franceschini, A. Riehle, and A. Le Nestour, "Directionally selective motion detection by insect neurons," in *Facets of Vision*, D. G. Stavenga and R. C. Hardie, Eds. Berlin, Germany: Springer-Verlag, 1989, pp. 360–390.

[159] R. Pierantoni, "A look into the cockpit of the fly. The architecture of the lobula plate," *Cell Tissue Res.*, vol. 171, pp. 101–122, 1976.

[160] L. G. Bishop, D. G. Keehn, and G. D. McCann, "Motion detection by interneurons of optic lobes and brain of the flies Calliphora phaenicia and Musca domestica," *J. Neurophys.*, vol. 32, pp. 509–525, 1968.

[161] K. Hausen, "Functional characterisation and anatomical identification of motion sensitive neurons in the lobula plate of the blowfly Calliphora erythrocephala," *Z. Naturforschung C*, vol. 31, pp. 629–633, 1976.

[162] R. Hengstenberg, "Common visual response properties of giant vertical cells in the lobula plate of the blowfly Calliphora," *J. Comparative Physiol.*, vol. 149, pp. 179–193, 1982.

[163] H. G. Krapp, B. Hengstenberg, and R. Hengstenberg, "Dendritic structure and receptive-field organization of optic flow processing interneurons in the fly," *J. Neurophys.*, vol. 79, no. 4, pp. 1902–1917, 1998.

[164] K. Hausen, "The lobula-complex of the fly: Structure, function and significance in visual behaviour," in *Photoreception and Vision in Invertebrates*, M. A. Ali, Ed. New York, NY, USA: Plenum, 1984, pp. 523–559.

[165] K. Hausen and M. Egelhaaf, "Neural mechanisms of visual course control in insects," in *Facets of Vision*, R. C. Hardie and D. G. Stavenga, Eds. Berlin, Germany: Springer-Verlag, 1989, pp. 391–424.

[166] K. Hausen, "Decoding of retinal image flow in insects," in *Visual Motion and Its Role in the Stabilization of Gaze*, F. A. Miles and J. Wallman, Eds. Amsterdam, The Netherlands: Elsevier, 1993, pp. 203–235.

[167] B. Bausenwein, A. P. M. Dittrich, and K. P. Fishbach, "The optic lobe of Drosophila melanogaster II. Sorting of retinotopic pathways in the medulla," *Cell Tissue Res.*, vol. 267, pp. 17–28, 1992.

[168] A. K. Warzecha, R. Rosner, and J. Grewe, "Impact and sources of neuronal variability in the fly's motion vision pathway," *J. Physiol.*, vol. 107, pp. 26–30, 2013.

[169] M. V. Srinivasan and D. R. Dvorak, "Spatial processing of visual information in the movement-detecting pathway of the fly, Characteristics and functional significance," *J. Comparative Physiol. A*, vol. 140, pp. 1–23, 1980.

[170] H. Eckert, "Functional properties of the H1-neurone in the third optic ganglion of thye blowfly Phaenicia," *J. Comparative Physiol.*, vol. 135, pp. 29–39, 1980.

[171] J. H. van Hateren, R. Kern, G. Schwertgeger, and M. Egelhaaf, "Function and coding in the blowfly H1 neuron during naturalistic optic flow," *J. Neurosci.*, vol. 25, pp. 4343–4352, 2005.

[172] N. J. Strausfeld and U. K. Bassemir, "Lobula plate and ocellar interneurons converge onto a cluster of descending neurons leading to neck and leg motor neuropil in Calliphora erythrocephala," *Cell Tissue Res.*, vol. 240, pp. 617–640, 1985.

[173] N. J. Strausfeld, H. S Seyan, and J. J. Milde, "The neck motor system of the fly Calliphora erythrocephala 1. Muscles and motor neurons," *J. Comparative Physiol. A*, vol. 160, pp. 205–224, 1987.

[174] S. J. Huston and H. G. Krapp, "Visuomotor transformation in the fly gaze stabilization system," *PLoS Biol.*, vol. 6, pp. 1468–1478, 2008.

[175] A. Wertz, A. Borst, and J. Haag, "Nonlinear integration of binocular optic flow by DNOVS2, a descending neuron of the fly," *J. Neurosci.*, vol. 28, pp. 3131–3140, 2008.

[176] H. B. Barlow and B. Hill, "Selective sensitivity to direction of movement in ganglion cells of the rabbit retina," *Science*, vol. 139, pp. 412–414, 1963.

[177] H. B. Barlow and W. R. Levick, "Mechanisms of directionally selective units in rabbit's retina," *J. Physiol.*, vol. 178, pp. 477–504, 1965.

[178] S. Exner, "Experimentelle Untersuchung der einfachsten psysischen Prozesse," *Pflüger's ArchaPhysiology*, vol. 11, pp. 403–432, 1875.

[179] J. C. Tuthill, A. Nern, S. L. Holtz, G. M. Rubin, and M. B. Reiser, "Contributions of the 12 neuron classes in the fly lamina to motion vision," *Neuron*, vol. 79, pp. 128–140, Jul. 2013.

[180] F. Mura, N. Martin, and N. Franceschini, "Biologically inspired eye movements for the visually guided navigation of mobile robots," in *Proc. Eur. Symp. Artif. Neural Netw.*, M. Verleysen, Ed., 1996, pp. 135–147.

[181] E. Buchner., S. Buchner, and I. Bülthoff, "Deoxyglucose mapping of nervous activity induced in Drosophila brain by visual movement, I. Wildtype," *J. Comparative Physiol. A*, vol. 155, pp. 471–483, 1984.

[182] C. W. Oyster, "The analysis of image motion by the rabbit retina," *J. Physiol.*, vol. 199, pp. 613–635, 1968.

[183] K. Kirschfeld, "The visual system of the fly: Physiological optics and functional anatomy as related to behavior," in *The Neurosciences Fourth Study Programme*, F. O. Schmitt and F. G. Worden, Eds. Cambridge, MA, USA: MIT Press, 1979, pp. 297–310.

[184] F. H. Schuling, H. A. K. Masterbroek, R. Bult, and B. P. M. Lenting, "Properties of elementary movement detectors in the fly Calliphora erythrocephala," *J. Comparative Physiol. A*, vol. 165, pp. 179–192, 1989.

[185] A. Schmid and H. Bülthoff, "Using neuropharmacology to distinguish between excitatory and inhibitory movement detection mechanisms in the fly Calliphora erythrocephala," *Biol. Cybern.*, vol. 59, pp. 71–80, 1988.

[186] C. Gilbert, "Membrane conductance changes associated with the response of motion sensitive insect visual neurons," *Zeitschr. Naturforschung C*, vol. 45, pp. 1222–1224, 1991.

[187] M. Joesch, J. Plett, A. Borst, and D. Reiff, "Response properties of motion-sensitive visual interneuron's in the lobula plate of Drosophila melanogaster," *Current Biol.*, vol. 18, pp. 368–374, 2008.

[188] A. Borst, M. Egelhaaf, and J. Haag, "Mechanismss of dendritic integration underlying gain control in fly motion-sensitive interneurons," *J. Comp. Neurosci.*, vol. 2, pp. 5–18, 1995.

[189] V. Torre and T. Poggio, "Synaptic mechanism possibly underlying directional selectivity to motion," *Proc. Roy. Soc. Lond. B*, vol. 202, pp. 409–416, 1978.

[190] V. Castelluci and E. Kandel, "Presynaptic facilitation as a mechanism for behavioral sensitization in Aplysia," *Science*, vol. 194, pp. 1176–1178, 1976.

[191] M. Klein and E. R. Kandel, "Mechanism of calcium current modulation underlying presynaptic facilitation and behavioral sensitization in Aplysia," *Proc. Nat. Acad. Sci. USA*, vol. 77, pp. 6912–6916, 1980.

[192] R. A. Harris, D. O'Carroll, and S. Laughlin, "Adaptation and the temporal delay filter of fly motion detectors," *Vis. Res.*, vol. 39, pp. 2603–2613, 1999.

[193] R. Harris and D. C. O'Carroll, "Afterimages in fly motion vision," *Vis. Res.*, vol. 42, pp. 1701–1714, 2002.

[194] A. Borst, C. Reisenman, and J. Haag, "Adaptation of response transients in fly motion vision," *Vis. Res.*, vol. 43, pp. 1309–1322, 2003.

[195] A. Borst, J. Haag, and D. F. Reiff, "Fly motion vision," *Annu. Rev. Neurosci.*, vol. 33, pp. 49–70, 2010.

[196] T. Maddess and S. B. Laughlin, "Adaptation of the motion-sensitive neuron H1 is generated locally and governed by contrast frequency," *Proc. Roy. Soc. Lond. B*, vol. 225, pp. 251–275, 1985.

[197] S. Anstis and B. J. Rogers, "Illusory reversal of visual depth and movement during changes of contrast," *Vis. Res.*, vol. 15, pp. 957–961, 1975.

[198] R. Juston, L. Kerhuel, N. Franceschini, and S. Violett, "Hyperacute edge and bar detection in a bioinspired optical position sensing device," *IEEE/ASME Trans. Mechatron.*, 2013, DOI: 10.1109/TMECH.2013.2265983.

[199] M. Joesch, B. Schnell, S. V. Raghu, D. F. Reiff, and A. Borst, "ON and OFF pathways in Drosophila motion vision," *Nature*, vol. 468, pp. 300–304, 2010.

[200] S. Ullman, "Analysis of visual motion by biological and computer systems," *Computer*, vol. 14, no. 8, pp. 57–69, 1981.

[201] S. B. Laughlin, R. R. de Ruyter van Steveninck, and J. C. Anderson, "The metabolic cost of neural information," *Nature Neurosci.*, vol. 1, pp. 36–41, 1998.

[202] P. H. Schiller, J. H. Sandell, and J. R. H. Maunsell, "Function of the On and Off channels of the visual system," *Nature*, vol. 322, pp. 824–825, 1986.

[203] G. Westheimer, "The ON-OFF dichotomy in visual processing: From receptors to perception," *Progr. Retinal Eye Res.*, vol. 26, pp. 636–648, 2007.

[204] N. Franceschini, J. M. Pichon, and C. Blanes, "Rectified high-pass filtering in early motion detection," *Soc. Neurosci. Abstracts*, vol. 15, p. 1290, 1989.

[205] E. Ahissar and A. Arieli, "Figuring space by time," *Neuron*, vol. 32, pp. 185–201, 2001.

[206] D. F. Reiff, J. Plett, M. Mank, O. Griesbeck, and A. Borst, "Visualizing retinotopic half-wave rectified input to the motion detection circuitry of Drosophila," *Nature Neurosci.*, vol. 13, pp. 973–978, 2010.

[207] J. Rister, D. Pauls, B. Schnell, C. Y. Ting, C. H. Lee, I. Sinakevitch, J. Morante, N. J. Strausfeld, K. Ito, and M. Heisenberg, "Dissection of the peripheral motion channel in the visual system of Drosophila melanogaster," *Neuron*, vol. 56, pp. 155–170, 2007.

[208] A. Y. Katzov and T. R. Clandinin, "Motion processing streams in Drosophila are behaviorally specialized," *Neuron*, vol. 59, pp. 322–335, 2008.

[209] D. A. Clark, L. Bursztyn, M. A. Horowitz, M. J. Schnitzer, and T. R. Clandinin, "Defining the computational structure of the motion detector in Drosophila," *Neuron*, vol. 70, no. 6, pp. 1165–1117, 2011.

[210] N. J. Strausfeld and J. K. Lee, "Neuronal basis for parallel visula processing in the fly," *Vis. Neurosci.*, vol. 7, pp. 16–33, 1991.

[211] J. K. Douglass and N. J. Strausfeld, "Visual motion detection circuits in flies: Peripheral motion computation by identified small field retinotopic neurons," *J. Neurosci.*, vol. 15, pp. 5596–5611, 1995.

[212] J. K. Douglass and N. J. Strausfeld, "Visual motion-detection circuits in flies: Parallel direction- and non-direction-sensitive pathways between the medulla and lobula plate," *J. Neurosci.*, vol. 16, no. 15, pp. 4551–4562, 1996.

[213] B. Schnell, S. V. Raghu, A. Nern, and A. Borst, "Columnar cells necessary for motion responses of wide-field visual interneurons in Drosophila," *J. Comparative Physiol. A*, vol. 198, pp. 389–395, 2012.

[214] P. E. Coombe, M. V. Srinivasan, and R. G. Guy, "Are the large monopolar cells of the insect lamina on the optomotor pathway?" *J. Comparative Physiol. A*, vol. 166, pp. 23–35, 1989.

[215] D. W. Arnett, "Spatial and temporal integration properties of units in the first optic ganglion of dipterans," *J. Neurophys.*, vol. 35, pp. 429–444, 1972.

[216] N. M. Jansonius and H. van Hateren, "On spiking units in the first optic chiasm of the blowfly III: The sustaining unit," *J. Comparative Physiol.*, vol. 173, pp. 187–192, 1993.

[217] C. Blanes and L. Oufar, "Guidage visuel d'un robot mobile," B.E. thesis, Ecole Nat. Sup. Physique, Marseille, France, 1985.

[218] N. Franceschini, C. Blanes, and L. Oufar, "Passive non-contact optical velocity sensor," *Dossier Tech. ANVAR/DVAR*, vol. 51, p. 549, 1986.

[219] M. Pichon, C. Blanes, and N. Franceschini, "Visual guidance of a mobile robot equipped with a network of self-motion sensors," in *Mobile Robots IV*, vol. 1195, W. J. Wolfe and Chun, Ed. Bellingham, WA, USA: SPIE., 1989, , pp. 44–53.

[220] S. Viollet, F. Ruffier, T. Ray, M. Mehnouni, F. Aubépart, L. Kerhuel, and N. Franceschini , "Characteristics of three miniature bio-inspired optic flow sensors in natural environments," in *Proc. IEEE 4th Int. Conf. Sens. Technol. Appl.*, 2010, pp. 51–55.

[221] J. Kramer, R. Sarpeshkar, and C. Koch, "An analog VLSI velocity sensor," in *Proc. IEEE Int. Symp. Circuits Syst.*, Seattle, WA, USA, 1995, pp. 413–416.

[222] G. Indiveri, J. Kramer, and C. Koch, "System implementations of analog VLSI velocity sensors," *IEEE Micro*, vol. 16, no. 5, pp. 40–49, Oct. 1996.

[223] R. Moeckel and S. C. Liu, "Motion detection circuits for a time-to-travel algorithm," in *Proc. IEEE Int. Symp. Circuits Syst.*, 2007, pp. 3079–3082.

[224] C. Blanes, "Guidage visuel d'un robot mobile autonome d'inspiration bionique. Implémentation opto-électronique et réalisation du prototype," Ph.D. dissertation, Neurocybern. Lab, Marseille, Nat. Polytech. Inst., Grenoble, France, 1991.

[225] N. Franceschini, A. Riehle, and A. Le Nestour, "Properties of the integrated circuit mediating directional selectivity in a movement sensitive neuron," *Soc. Neurosci. Abstracts*, vol. 12, p. 859, 1986.

[226] M. Pudas, S. Viollet, F. Ruffier, A. Kruusing, S. Amic, S. Leppävuori, and N. Franceschini, "A miniature bio-inspired optic flow sensor based on low temperature co-fired ceramics (LTCC) technology," *Sens. Actuators A*, vol. 133, pp. 88–95, 2007.

[227] T. Delbrück and C. Mead, "Adaptive photoreceptor with wide dynamic range," in *Proc. IEEE Int. Symp. Circuits Syst.*, 1994, vol. 4, pp. 339–342.

[228] F. Aubépart, M. Ménouni, T. Loubignac, B. Dinkelspieler, and N. Franceschini,

"Capteur de flux optique basé sur une rétine intégrée et un FPGA," in *Colloque Interdisciplinaire en Instrumentation*. Paris, France: Hermès, 2007, pp. 508–520.

[229] F. Ruffier, S. Viollet, S. Amic, N. Franceschini, and N., "Bio-inspired optical flow circuits for the visual guidance of micro-air vehicles," in *Proc. IEEE Int. Symp. Circuits Syst.*, Bangkok, Thailand, 2003, pp. 846–849.

[230] F. Aubépart, M. El Farji, and N. Franceschini, "FPGA implémentation of elementary motion detectors for the visual guidance of micro-air vehicles," in *Proc. IEEE Symp. Ind. Electron.*, 2004, pp. 61–76.

[231] G. K. Taylor and H. G. Krapp, "Sensory systems and flight stability: What do insects measure and why?" in *Advances in Insect Physiology*, vol. 34, J. Casas and S. J. Simpson, Eds. Amsterdam, The Netherlands: Elsevier, 2007, pp. 231–316.

[232] N. Franceschini, J. M. Pichon, and C. Blanes, "Real time visuomotor control: From flies to robots," in *Proc. IEEE Conf. Adv. Robot.*, Pisa, Italy, 1991, pp. 931–935.

[233] N. Franceschini, J. Pichon, and C. Blanes, "Bionics of Visuo-Motor Control," in *Evolutionary Robotics: From Intelligent Robots to Artificial Life*, T. Gomi, Ed. Toronto, ON, Canada: AAAI Books, 1997, pp. 49–67.

[234] C. Schilstra and C. J. H. van Hateren, "Blowfly flight and optic flow 1/Thorax kinematics and flight dynamics," *J. Exp. Biol.*, vol. 202, pp. 1481–1490, 1999.

[235] L. F. Tammero and M. Dickinson, "The influence of visual landscape on the free flight behavior of the fruitfly Drosophila melanogaster," *J. Exp. Biol.*, vol. 205, pp. 327–343, 2002.

[236] M. Egelhaaf, R. Kern, J. P. Lindemann, E. Braun, and B. Geurten, "Active vision in blowflies: Strategies and mechanisms of spatial orientation," in *Flying Insects and Robots*, D. Floreano, J.-C. Zufferey, M. V. Srinivasan, and C. Ellington, Eds. Berlin, Germany: Springer-Verlag, 2009, pp. 51–61.

[237] J. Gibson, P. Olum, and F. Rosenblatt, "Parallax and perspective during aircraft landings," *Amer. J. Psychol.*, vol. 68, pp. 372–385, 1955.

[238] J. J. Koenderink, "Optic flow," *Vis. Res.*, vol. 26, no. 1, pp. 161–179, 1986.

[239] M. Zaretsky and C. H. F. Rowell, "Saccadic suppression by corollary discharge in the locust," *Nature*, vol. 280, no. 5723, pp. 583–585, 1979.

[240] R. Pfeifer, M. Lungarella, and F. Iida, "Self-organization, embodiment, biologically inspired robotics," *Science*, vol. 318, no. 5853, pp. 1088–1093, 2007.

[241] N. Martin and N. Franceschini, "Obstacle avoidance and speed control in a mobile vehicle equipped with a compound eye," in *Intelligent Vehicles*, I. Masaki, Ed. Cambridge, MA, USA: MIT Press, 1994, pp. 381–386.

[242] F. Ruffier and N. Franceschini, "Optic flow regulation over a moving platform: A tethered aerial robot evaluated terrain following and target landing," *J. Intell. Robot. Syst.*, 2014, in press.

[243] N. Franceschini, F. Ruffier, and J. Serres, "A bio-Inspired flying robot sheds light on insect piloting abilities," *Current Biol.*, vol. 17, no. 4, pp. 329–335, 2007.

[244] F. Ruffier and N. Franceschini, "Visually guided micro-aerial vehicle: Automatic take off, terrain following, landing and wind reaction," in *Proc. IEEE Int. Conf. Robot. Autom.*, New Orleans, LA, USA, 2004, pp. 2339–2346.

[245] F. Ruffier and N. Franceschini, "Optic flow regulation: The key to aircraft automatic guidance," *Robot. Autonom. Syst.*, vol. 50, no. 4, pp. 177–194, 2005.

[246] J. Serres, D. Dray, F. Ruffier, and N. Franceschini, "A vision-based autopilot for a miniature air vehicle: Joint speed control and lateral obstacle avoidance," *Autonom. Robots*, vol. 25, no. 1, pp. 103–122, 2008.

[247] F. L. Roubieu, J. Serres, F. Colonnier, N. Franceschini, S. Viollet, and F. Ruffier, "A biomimetic vision-based hovercraft accounts for bees' complex behaviour in various corridors," *Bioinspiration Biomimetics*, vol. 9, no. 3, 2014.

[248] W. H. Kirchner and M. V. Srinivasan, "Freely flying honeybees use image motion to estimate distance," *Naturwissenschaften*, vol. 76, pp. 281–282, 1989.

[249] J. Serres, G. Masson, F. Ruffier, and N. Franceschini, "A bee in the corridor: Centering and wall-following," *Naturwissenschaften*, vol. 95, pp. 1181–1187, 2008.

[250] G. Portelli, F. Ruffier, and N. Franceschini, "Honeybees change their height to restore their optic flow," *J. Comparative Physiol. A*, vol. 196, pp. 307–313, 2010.

[251] M. V. Srinivasan, S. Zhang, J. Chahl, F. Barth, and S. Venkatesh, "How honeybees make grazing landings on flat surfaces," *Biol. Cybern.*, vol. 83, no. 3, pp. 171–183, 2000.

[252] H. Heran and M. Lindauer, "Windkompensation und Seitenwindkorrektur der Bienen beim Flug über Wasser," *J. Comparative Physiol. A*, vol. 47, no. 1, pp. 39–55, 1963.

[253] M. V. Srinivasan, S. W. Zhang, M. Lehrer, and T. S. Collett, "Honeybee navigation en route to the goal: Visual flight control and odometry," *J. Exp. Biol.*, vol. 199, no. 1, pp. 237–244, 1996.

[254] F. Mura and N. Franceschini, "Biologically inspired 'retinal scanning' enhances motion perception of a mobile robot," in *1st Europe-Asia Congress on Mechatronics*, vol. 3, A. Bourjault and S. Hata, Eds. Besançon, France: ENSM, 1996, , pp. 934–940.

[255] S. Viollet and N. Franceschini, "Biologically inspired visual scanning sensor for stabilization and tracking," in *Proc. IEEE Int. Conf. Intell. Robots Syst.*, Kyon-gyu, Korea, 1999, vol. 1, pp. 204–209.

[256] S. Viollet and N. Franceschini, "A hyperacute optical position sensor based on biomimetic retinal microscanning," *Sens. Actuators A*, vol. 160, pp. 60–68, 2010.

[257] G. Westheimer, "Visual hyperacuity," in Sensory Physiology, vol. 1, D. Ottoson, Ed. Berlin, Germany: Springer-Verlag, 1981, pp. 1–30.

[258] S. Viollet, J. Michelis, and N. Franceschini, "Toward a bio-inspired nonemissive powerline detection system," in *Proc. 32nd Eur. Rotorcraft Forum*, Maastricht, The Netherlands, 2006, paper AD09.

[259] S. Viollet and N. Franceschini, "Super-accurate visual control of an aerial minirobot," in *Autonomous Minirobots for Research and Edutainment (AMIRE 01)*, U. Rückert, J. Sitte, and U. Witkowski, Eds. Paderborn, Germany: H. Nixdorf Inst., 2001, pp. 215–224.

[260] N. Franceschini, "Visual guidance based on optic flow: A biorobotic approach," *J. Physiol.*, vol. 98, no. 1–3, pp. 281–292, 2004.

[261] D. Sandeman, "Head movements in flies (Calliphora) produced by deflexion of the halteres," *J. Exp. Biol.*, vol. 85, no. 1, pp. 43–60, 1980.

[262] R. Hengstenberg, "Mechanosensory control of compensatory head roll during flight in the blowfly Calliphora erythrocephala meig," *J. Comparative Physiol. A*, vol. 163, pp. 151–165, 1988.

[263] W. P. Chan, F. Prete, and M. H. Dickinson, "Visual input to the efferent control system of a fly's « gyroscope »," *Science*, vol. 280, no. 5361, pp. 289–292, 1998.

[264] C. Schilstra and J. H. van Hateren, "Stabilizing gaze in flying blowflies," *Nature*, vol. 395, no. 6703, p. 654, 1998.

[265] J. Zeil, N. Boeddeker, and J. M. Hemmi, "Vision and the organization of behaviour," *Current Biol.*, vol. 18, no. 8, pp. R320–R323, 2008.

[266] F. Miles and D. Wallman, *Visual Motion and Its Role in the Stabilisation of Gaze*, F. A. Miles and J. Wallman, Eds. Amsterdam, The Netherlands: Elsevier, 1993.

[267] M. Huterer and K. E. Cullen, "Vestibulo-ocular reflex dynamics during high-frequency and high acceleration rotations of the head on body in rhesus monkey," *J. Neurophysiol.*, vol. 88, pp. 13–28, 2002.

[268] S. Viollet and N. Franceschini, "A high speed gaze control system based on the vestibulo-ocular reflex," *Robot. Autonom. Syst.*, vol. 50, no. 4, pp. 147–161, 2005.

[269] L. Kerhuel, S. Viollet, and N. Franceschini, "Steering by gazing: An efficient biomimetic control strategy for visually guided micro aerial vehicles," *IEEE Trans. Robot.*, vol. 26, no. 2, pp. 307–319, Apr. 2010.

[270] S. Ushida, K. Yoshimi, T. Okatani, and K. Deguchi, "The importance of gaze control mechanisms on vision-based control of a biped robot," in *Proc. IEEE/RSJ Int. Conf. Intell. Robots Syst.*, 2006, pp. 4447–4452.

[271] F. Jacob, "Evolution and tinkering," *Science*, vol. 196, no. 4295, pp. 1161–1166, 1977.

[272] J. P. C. Dumont and R. M. Robertson, "Neuronal circuits: An evolutionary perspective," *Science*, vol. 233, pp. 849–853, 1986.

[273] S. Shaw, "Early visual processing in insects," *J. Exp. Biol.*, vol. 112, pp. 225–251, 1984.

[274] M. Egelhaaf and A. Borst, "Are there separate ON and OFF channels in fly motion vision?" *Vis. Neurosci.*, vol. 8, pp. 151–164, 1992.

[275] R. Rosner R, M. Egelhaaf, and M. A. K. Warzecha, "Behavioural state affects motion-sensitive neurones in the fly visual system," *J. Exp. Biol.*, vol. 213, pp. 331–338, 2010.

[276] K. D. Longden and H. Krapp, "Sensory neurophysiology: Motion vision during motor action," *Current Biol.*, vol. 21, no. 17, pp. R.650–R652, 2011.

[277] C. A. Mead and M. Mahowald, "A silicon model of early visual processing," in *Computational Neuroscience*, E. L. Schwartz, Ed. Cambridge, MA, USA: MIT Press, 1989, pp. 331–339.

[278] D. Floreano, R. Pericet-Camara, S. Viollet, F. Ruffier, A. Brückner, R. Leitel, W. Buss, M. Menouni, F. Expert, R. Juston, M. K. Dobrzynski, G. L'Eplattenier, F. Recktenwald, H. A. Mallot, and

N. Franceschini, "Miniature curved artificial compound eyes," *Proc. Nat. Acad. Sci. USA*, vol. 110, pp. 9267–9272, Jun. 2013.

[279] S. B. Laughlin and M. Weckström, "Fast and slow photoreceptors—A comparative study of the functional diversity of coding and conductances in the Diptera," *J. Comparative Physiol. A*, vol. 172, no. 5, pp. 593–609, 1993.

[280] Y. M. Song, Y. Xie, V. Malyarchuk, J. Xiao, I. Jung, K. J. Choi, Z. Liu, H. Park, C. Lu, R. Kim, R. Li, K. B. Crozier, Y. Huang, and J. A. Rogers, "Digital cameras with designs inspired by the arthropod eye," *Nature*, vol. 497, no. 7447, pp. 95–99, 2013.

[281] R. Bajcsy, "Active perception versus passive perception," in *Proc. 3rd IEEE Workshop Comput. Vis., Represent. Control*, Bellaire, MI, USA, 1985, vol. 8, pp. 55–59.

[282] D. Ballard, "Animate vision," *Artif. Intell.*, vol. 48, no. 1, pp. 57–86, 1991.

[283] Y. Aloimonos, *Active Perception*. Mahwah, NJ, USA: Lawrence Erlbaum, 1993.

[284] N. Franceschini, "Towards automatic visual guidance of aerospace vehicles: From insects to robots," *Acta Futura*, vol. 3, pp. 15–29, 2009.

[285] F. Valette, F. Ruffier, S. Viollet, and T. Seidl, "Biomimetic optic flow sensing applied to a lunar landing scenario," in *Proc. IEEE Int. Conf. Robots Autom.*, Anchorage, AK, USA, 2010, pp. 2253–2260.

[286] D. Izzo, N. Weiss, and T. Seidl, "Constant-optic-flow lunar landing: Optimality and guidance," *J. Guid. Control Dyn.*, vol. 34, no. 5, pp. 1383–1395, 2011.

[287] T. Raharijaona, G. Sabiron, S. Viollet, N. Franceschini, and F. Ruffier, "Bio-inspired landing approaches and their potential use on extraterrestrial bodies," in *Asteroids*, V. Badescu, Ed. Berlin, Germany: Springer-Verlag, 2013, ch. 9, pp. 221–246.

[288] J. Chahl, S. Thakoor, N. Le Bouffant, G. Stange, and M. V. Srinivasan, "Bioinspired engineering of exploration systems: A horizon sensor/attitude reference system based on the dragonfly ocelli for *Mars exploration applications*," *J. Robot. Syst.*, vol. 20, no. 1, pp. 35–42, 2003.

[289] T. Gandhi, M. Yang, R. Kasturi, O. Coraor, and L. J. McCandless, "Detection of obstacles in flight path of an aircraft," *IEEE Trans. Aerosp. Electron. Syst.*, vol. 39, no. 1, pp. 176–191, Jan. 2003.

[290] L. Kerhuel, S. Viollet, and N. Franceschini, "The VODKA sensor: A bio-inspired hyperacute optical position sensing device," *IEEE Sens. J.*, vol. 12, no. 2, pp. 315–324, Feb. 2012.

[291] M. Shimomura and T. Shimozawa, *New Generation Nanomaterials Inspired by Insects*. Tokyo, Japan: NTS, 2008.

[292] K. P. Hadeler, "In Memory of Dezsö Varju, News Archive of the Werner Reichardt Center for Integrative Neuroscience," 2013. [Online]. Available: http://www.cin.uni-tuebingen.de/press-amp-news/latest.php?

ABOUT THE AUTHOR

Nicolas Franceschini was born in Mâcon, France, in 1942. He was awarded the B.E. degree in electronic engineering, the M.S. degree in control engineering, and the Doctorat d'Etat degree in physics from the National Polytechnic Institute and University of Grenoble, Grenoble, France, in 1964, 1965, and 1972, respectively.

The paper entitled "What the frog's eye tells the frog's brain" by Lettvin *et al*. [1] prompted him to switch from physics to Neuroscience and Behavioral Science. He worked as a Research Assistant at the Max-Planck Institute for Biological Cybernetics in Tübingen, Germany until 1979. He was then appointed as a Research Director at the C.N.R.S. in France and set up the Neurocybernetics Laboratory—and later the Biorobotics Laboratory— in Marseille. His research interests include neural information processing, vision, eye movements, microoptics, neuromorphic circuits, sensory-motor control systems, biologically-inspired robots and insect-inspired autopilots. He has published over 170 papers in the fields of neurobiology, behavioral science and biorobotics, and given about 160 invited lectures at international conferences. He was a Visiting Scientist at the University of Sherbrooke, Sherbrooke, QC, Canada; KEIO University School of Medicine, Tokyo, Japan; the Australian National University, Canberra, A.C.T., Australia; the Max-Planck Institute for Biological Cybernetics, Tübingen, Germany; the University of Ulm, Ulm, Germany; and the ElectroTechnical Laboratory (E.T.L.), Tsukuba, Japan; and was a reviewer for various French and foreign organisations, including the New Energy and Industrial Technology Development Organization (NEDO, Japan), RIKEN Brain Science Institute and RIKEN Biomimetic Control Research Centre, the National Science Foundation (NSF, USA) RS (UK), the National Security Evaluation Corporation (NSEC, Canada), the Human Frontier Science Program (HFSP), and European Union programs.

Dr. Franceschini has received several honors in the fields of both neuroscience and robotics. With his colleagues, he has received three IEEE paper awards and the prize awarded by the journal *La Recherche*. He has also received the C.N.R.S silver medal in Life Science, the Charles-Louis de Saulces de Freycinet prize and the Grand Prize in Integrative Neuroscience awarded by the French Academy of Science. In 1992 he was awarded the international LVMH (Louis-Vuitton-Moët-Hennessy) prize, along with Richard Axel and Linda Buck. He has largely contributed to initiating and developing the field of Biorobotics since 1985. He was elected as a member of the *Academia Europaea* in 1996.